Final Report

RI 98-032

EXPERIMENTAL TESTING AND MODELING OF A FRP BRIDGE

MISSOURI DEPARTMENT OF TRANSPORTATION
RESEARCH, DEVELOPMENT AND TECHNOLOGY

By:
K. Chandrashekhara
Department of Mechanical and Aerospace Engineering and Engineering Mechanics
And
Antonio Nanni
Department of Civil Engineering, Center For Infrastructure Engineering Studies
UNIVERSITY OF MISSORI –ROLLA, ROLLA, MISSOURI

JEFFERSON CITY, MISSOURI
DATE SUBMITTED: December 2000

TECHNICAL REPORT DOCUMENTATION PAGE

1. Report No. RDT 00-016	2. Government Accession No.	3. Recipient's Catalog No.
4. Title and Subtitle Experimental Testing and Modeling of a FRP Bridge		5. Report Date December 2000 6. Performing Organization Code RDT 00-016 / RI 98-032
7. Author(s) K. Chandrashekhara and Antonio Nanni		8. Performing Organization Report No.
9. Performing Organization Name and Address Center for Infrastructure Engineering Studies University of Missouri-Rolla Rolla, MO 65409		10. Work Unit No. 11. Contract or Grant No.
12. Sponsoring Agency Name and Address Missouri Department of Transportation Research, Development and Technology P. O. Box 270-Jefferson City, MO 65102		13. Type of Report and Period Covered Final Report 14. Sponsoring Agency Code

15. Supplementary Notes

The investigation was conducted in cooperation with the U. S. Department of Transportation, Federal Highway Administration.

16. Abstract

An all-composite bridge, 9.14 m (30 ft) long and 2.74 m (9 ft) wide, has been designed and built. The bridge was constructed using pultruded glass and carbon tubes. The performance of pultruded tubes, tube assembly, and quarter portion of the bridge deck were evaluated. The fatigue test on a quarter portion of the bridge served as a simple baseline of the long-term durability of the composite deck. The sample showed almost no reduction in stiffness or strength after 2 million cycles of fatigue loading in excess of the design load. The bridge was installed at UMR campus on July 29, 2000. The bridge is equipped with integral fiber optic sensors, and the response of the bridge will be remotely monitored.

17. Key Words FRP, Composite Material, Pultruded Tubes, Tube Assembly, Bridge Deck	18. Distribution Statement No restrictions. This document is available to the public through National Technical Information Center, Springfield, Virginia 22161

19. Security Classification (of this report) Unclassified	20. Security Classification (of this page) Unclassified	21. No. of Pages	22. Price

Form DOT F 1700.7 (06/98)

EXECUTIVE SUMMARY

The purpose of this project is to evaluate the performance of an all composite bridge. An extensive experimental study and finite element analysis were carried out to obtain and compare properties (stiffness, strength, failure modes) of 76 mm (3 in) square hollow pultruded glass FRP tubes and their assemblies. Tube assemblies were used in the fabrication of a bridge deck designed for H-20 truckloads as specified by the American Association of State Highway and Transportation Officials (AASHTO). The bridge is 9.14 m (30 ft) long and is 2.74 m (9 ft) wide. All the coupons were tested under three- or four-point bending. Experimental results show excellent linear elastic behavior up to failure and are in good agreement with finite element solutions. A quarter portion of the full-size bridge deck was then tested for its structural performance under design and fatigue loading and also for ultimate load capacity to evaluate the bridge response. The characteristics of the full-size bridge deck were determined by analyzing the performed tests. The bridge was installed at the UMR campus in July 2000.

Based on results of the present research, all-composite bridge decks made of pultruded glass and carbon FRP tubes are judged to be a suitable replacement for short span bridges made of conventional materials.

ACKNOWLEDGMENTS

The funding of this project was shared by the Missouri Department of Transportation, National Science Foundation, Lemay Center for Composites Technology, and University Transportation Center of University of Missouri – Rolla. The authors would like to thank Mr. John Unser of Composite Product Inc. for providing the samples, and Mr. Prakash Kumar, Graduate Research Assistant at University of Missouri-Rolla.

TABLE OF CONTENTS

Page

LIST OF ILLUSTRATIONS

Figure Page

1. INTRODUCTION

The construction and infrastructure industry has used conventional composite materials (e.g. reinforced concrete) for many years because they perform better than the constituents themselves and better than competing homogeneous materials. Advanced composite materials like Fiber Reinforced Polymer (FRP) composites have been increasingly gaining the interest of researchers and engineers as attractive alternatives to conventional materials used in civil engineering due to their unique properties such as high strength-to-weight ratio, excellent corrosion and fatigue resistance, manufacturing flexibility, tailoring of the material to specific applications, modular construction and overall environmental durability. Several writers (Liskey (1991), Aref and Parsons (1996), and Karbhari et al. (1997)) have documented the deteriorating condition of bridges and other infrastructure facilities all over the United States in recent years. This growing concern has prompted civil engineers to consider alternatives for conventional materials. In this effort to find a way to extend the life of structures and to make them easier to construct and maintain, the use of FRP materials has been recommended (Zureick et al. (1995)). One of the present areas of emphasis is the use of composite materials for the fabrication of lightweight bridge decks that can be deployed for replacement of deteriorating ones or for the erection of new ones. However, the application of composite materials to infrastructure has been limited due to the lack of industry-recognized design criteria and standards and standardized test methods (Ballinger (1990)). The introduction of mass-produced FRP structural shapes in bridges and highway applications dictates the necessity for a more complete understanding of the

static behavior of these shapes for the types of load and strain ranges that are typically anticipated so as to optimize the design and evaluation techniques.

Bank (1989) showed that because of the difference in mechanical properties between a full-size Glass Fiber Reinforced Polymer (GFRP) beam and a GFRP coupon, the full-size beam flexural modulus of pultruded GFRP beams is different from the coupon flexural modulus, and the coupon flexural modulus also differs from the coupon longitudinal modulus. Due to these differences, it becomes necessary to conduct tests and study the behavior of full-size GFRP beams at component or beam level in addition to coupon level. Nagaraj and Rao (1993) have characterized the behavior of pultruded GFRP box beams under static and fatigue or cyclic bending loads. The tests showed that the shear and interfacial slip between adjacent layers had significant influence on deflection and strain measurements. Davalos and Qiao (1997) conducted a combined analytical and experimental evaluation of flexural-torsional and lateral-distortional buckling of FRP composite wide-flange beams. They also showed that in general buckling and deflections limits tend to be the governing design criteria for current FRP shapes. The structural efficiency of pultruded FRP components and systems in terms of joint efficiency, transverse load distribution, composite action between FRP components, and maximum deflections and stresses was analyzed by Sotiropoulos et al. (1994) by conducting experiments at the coupon level. Structural performance of individual FRP components was established through three- and four-point bending tests. Barbero et al. (1991) gave a theoretical determination of the ultimate bending strength of GFRP beams produced by pultrusion process. Several I-beams and box beams were tested under bending and the failure modes have been described. The simultaneous determination of

flexural and shear moduli using an experimental method by three-point bending has been done by Fisher et al. (1981). The behavior of pultruded GFRP wide flange and box beams under static loads has been studied by Nagaraj and Rao (1997). They also developed theoretical methods for bending and shear stiffness computations and compared them with experimental results.

In the present study, the performance evaluation of pultruded hollow tubes, tube assembly and an all-composite bridge deck are investigated. The focus of the first part of the study is to provide structural design information pertaining to mechanical properties and failure modes of square hollow pultruded tubes made of glass fibers in vinyl ester resin when used as a primary load bearing member. The study also investigates the influence of shear, buckling, initial crookedness, and manufacturing defects (material non-uniformity or asymmetry) on the structural behavior of GFRP hollow tubes. Special emphasis is given to understanding the modes of failure under static loading. Several coupons consisting of single, double and a four-layered tube assembly were tested under static flexural loading. The coupons consisted of 76 mm (3 in) square hollow pultruded GFRP tubes with a thickness of 6.35 mm (0.25 in). The coupons were tested to failure under flexural loading and data obtained for deflection and strain were evaluated. The results obtained were compared with those from the finite element analysis (FEA). The stress distribution and modes of failure, determined by the tests, were verified numerically. The validation model allows one to investigate feasibility of the design and to predict the behavior of the bridge. The knowledge and data gained from these tests will be used to analyze the response of the GFRP composite materials and of various assemblies built out of it, especially with regard to bridge deck applications.

The purpose of the second part is to present fatigue and strength experimental qualifications performed for an all-composite bridge deck. This bridge deck, made up of fiber-reinforced polymer (FRP) was installed on the campus at University of Missouri at Rolla. The materials used for the fabrication of this 9.14 m (30 ft) long by 2.74 m (9 ft) wide deck were 76 mm (3 in) pultruded square hollow glass and carbon FRP tubes of varying lengths. These tubes were bonded using an epoxy adhesive and mechanically fastened together using screws in seven different layers to form the bridge deck with tubes running both longitudinal and transverse to the traffic direction. The cross-section of the deck was in the form of four identical I-beams running along the length of the bridge. Fatigue and failure tests were conducted on a 9.14 m (30 ft) long by 610 mm (2 ft) wide prototype deck sample, equivalent to a quarter portion of the bridge deck. The loads for these tests were computed so as to meet American Association of State Highway and Transportation Officials (AASHTO) H-20 truckload requirements based on strength and maximum deflection. The sample was fatigued to 2 million cycles under service loading and a nominal frequency of 4 Hz. Stiffness changes were monitored by periodically interrupting the run to perform a quasi-static test to service load. Results from these tests indicated no loss in stiffness up to 2 million cycles. Following the fatigue testing, the test sample was tested to failure and no loss in strength was observed. The testing program, specimen detail, experimental setup and instrumentation, testing procedure, and the results of these tests are discussed in detail. A finite-element model of the laboratory test was also developed. The results from the model showed good correlation to deflections and longitudinal strains measured during the tests. The design of the bridge deck has been discussed in detail.

2. TESTING AND EVALUATION OF COMPONENTS FOR A COMPOSITE BRIDGE DECK

2.1 DETAILS OF THE GFRP TUBES USED

The GFRP tubes used for the tests were manufactured using a pultrusion process. This process involves the pulling of reinforcing fibers and resin matrix through a die that shape and cures the material. Pultruded composite members are being used extensively as beams for structural applications. It offers many distinct advantages for mass production of FRP tubes to be used for the composite bridge deck, such as low operating costs, high production rate, product reproducibility and dimensional tolerances. Dry tows of FRP were pulled through a resin bath, before being drawn into a die. Standard vinyl ester resin was used for this application. Aluminum Trihydrate (ATH), a common flame retardant, was used along with the resin. In case of fire, ATH releases water and thus prevents the fire from spreading or damaging the structure. The cured tubes were pulled out of the die using a mechanism of two intermittent clamps to give a continuous pulling action. Each of these clamps grips on the forward stroke and releases on the backstroke. A cut-off saw was used to obtain tubes of appropriate lengths.

The tubes manufactured for testing had a fiber volume fraction of fifty-five percent. The fibers consist of continuous strand fiberglass mat and fiberglass rovings with fifty percent by volume fiberglass mat and fifty percent fiberglass roving. The mat was laid down on the outside, middle and inside of the tube while the rest consisted of fiberglass rovings. The unidirectional continuous strand fiberglass rovings, laid down along the axis of the tube, were responsible for providing the longitudinal mechanical properties, while the continuous strand fiberglass mat provided the transverse properties of the tubes (Agarwal and Broutman (1990)). Coupons were cut out from a tube in 0^0,

90^0 and 45^0 fiber orientation, were tested in tension and the moduli were determined for all the three cases. This helped to determine the material properties of the GFRP composite used for manufacturing the tubes and to verify the accuracy of the micro-mechanics model used to predict composite properties from the material properties of the constituents (fibers and resin). The modulus in the 0^0, 90^0 and 45^0 fiber directions were 21.38 GPa (3,100 ksi), 8.2 GPa (1,190 ksi) and 7.05 GPa (1,023 ksi) respectively. The modulus in 90^0 fiber direction was higher than that along the 45^0 due to the presence of layers of mat.

The present study was conducted on three different specimens tested under three- or four-point bending configuration. The essential component of each of these samples consisted of pultruded hollow GFRP tubes having a square cross-section of 76 mm (3 in) and a thickness of 6.35 mm (0.25 in). The specimens and their assembling techniques are described below.

2.1.1 SINGLE GFRP TUBE

The first specimen consists of single square hollow tubes having a length of 2.44 m (8 ft). The smallest component of the proposed deck is a single FRP tube, several of which are bonded together to build the deck, and so it becomes necessary to know their mechanical properties and failure modes. Several such coupons were tested under identical flexural loading and boundary conditions, and results of one of them have been discussed in the following sections.

2.1.2 DOUBLE TUBE ASSEMBLY

The next set of samples were made by bonding together two 2.44 m (8 ft) long GFRP tubes longitudinally along one of their surfaces using an adhesive to form a double tube assembly. Each of the tubes was of the same dimensions as that of the single tubes described before. This test was performed to investigate behavior of the GFRP tubes when bonded together using an adhesive into one integral piece. Samples were prepared using three different types of adhesives. The bonding surface of each tube was scuff sanded and washed with acetone using a clean rag. A thin layer of adhesive was applied to a surface of one of the tubes. The second tube was c-clamped to the first. The squeezed out adhesive was cleaned off. The assembly was allowed to cure as per the manufacturer's directions. Three different types of adhesives were investigated and it was observed that Hysol 9460 epoxy gave the best bonding surface between the tubes.

2.1.3 FOUR-LAYERED TUBE ASSEMBLY

The third sample in this series of tests consisted of an assembly of four layers of GFRP tubes. This assembly resembles an element of a full composite bridge deck having four layers of tubes. The overall philosophy of this test was to determine the characteristics of a large-scale bridge deck by performing tests on smaller components or assemblies that go into its fabrication. The first and third layers from the top of the sample consisted of thirty-two 304.8 mm (1 ft) long GFRP tubes in both layers having the same cross-section as the single tubes. The second and the fourth layers from the top of the sample consisted of four GFRP tubes in each layer, similar in dimensions to the single tubes described before. Hysol 9460 epoxy was used as the adhesive. The assembly of the

tubes and the overall dimension of the sample is shown in Figure 1. The full structure was assembled in two steps. The bottom most layer was assembled first. Four 2.44 m (8 ft) GFRP tubes were scuff sanded and washed with acetone. A thin layer of adhesive was applied to them and they were held together using bar clamps to bond them together. The second layer from the bottom, consisting of thirty-two 304.8 mm (1 ft) long tubes was added to the top of the first layer. The first tube was c-clamped to the lower layer and the next tube was c-clamped to this tube. As the tubes were added the c-clamp was moved to the next tube. A piece of plywood was placed on top of this layer of tubes and several heavy weights were placed over it. Another similar two-layer structure was assembled separately using the same technique and both the assemblies were allowed to cure overnight. Both the two-layer structures were bonded together using a thin layer of adhesive to form a single four-layered structure with dimensions of 2.44 m x 304.8 mm x 304.8 mm (8 ft x 1 ft x 1 ft). The whole assembly was cured for 72 hours prior to testing. The first and the third layers from the top were mainly responsible for distributing the load to the second and fourth layers that were the main load-bearing members.

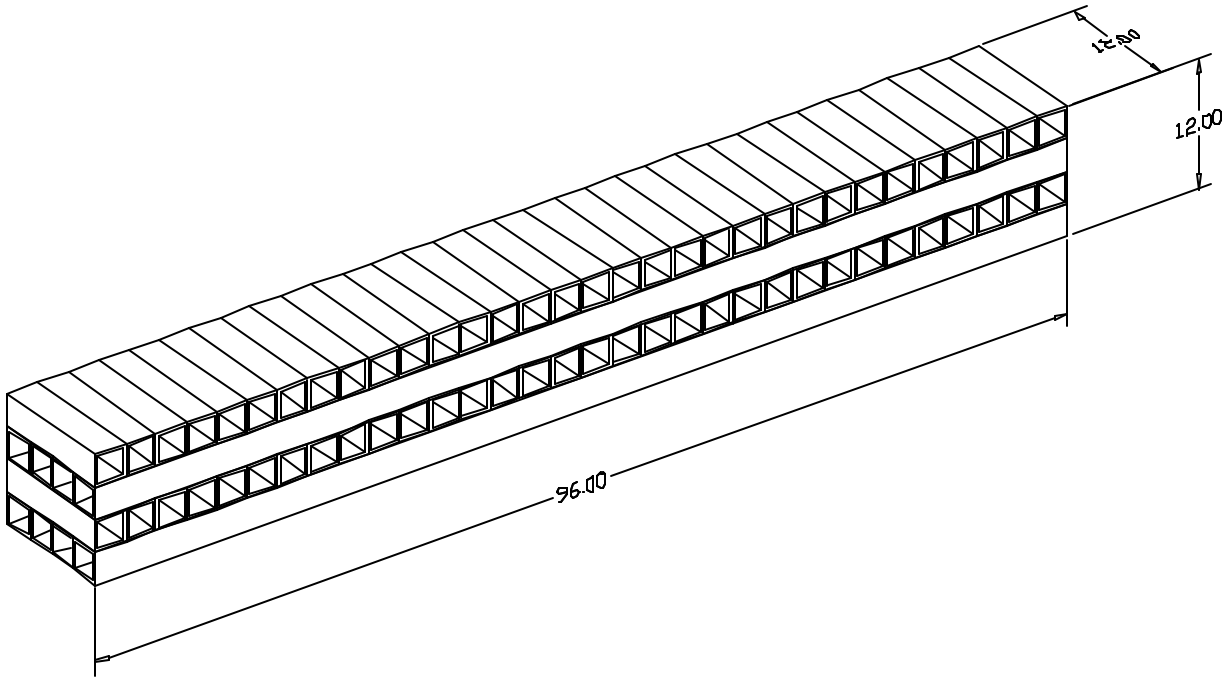

Figure 1: Four-layered GFRP tube assembly

Note: 1 in = 25.4 mm.

All dimensions are in inches

2.2 EXPERIMENTAL SETUP AND INSTRUMENTATION

The single tubes and the double tube assemblies were tested in four-point bending configuration, while the four-layered tube assembly was tested in three-point bending configuration. The samples were tested in simply supported boundary conditions and were placed on rollers on both the ends spaced at a distance of 2.13 mm (7 ft) so that the sample extended 152.4 mm (6 in) beyond the support rollers at each end. To alleviate the effects of surface imperfections and assure uniform reaction forces, a piece of plywood was placed between the steel plates and the bottom surface of the samples. Load was applied using a Baldwin Universal Testing machine with the centers of sample and the loading machine aligned together. For the four-point bending test, the two points of loading were 152.4 mm (6 in) on both sides of the center of the sample. A 12.7 mm (0.5 in) thick steel plate was placed under each point of loading so as to distribute the load over a wider area of the sample. A 89 kN (20,000 lb) load cell was used to measure the load. In the three-point bending test on the four-layered tube assembly, the center load was imposed through a 20.3 mm (0.8 in) thick by 304.8 mm (1 ft) square steel plate with a plywood pad between the sample top surface and the steel plate. A 222 kN (50,000 lb) load cell was used to measure the load for this case.

The instrumentation of the samples consisted of LVDTs (Linear variable differential transformers) to measure displacement and 6 mm (0.24 in) long 120 ohms electrical resistance strain gages for strain measurement. Three LVDTs were attached to each of the samples, two at the points of support and one at the mid-span, to measure the linear deflection. Two strain gages were attached to each of the samples to measure the

strain developed. In case of single tube and double tube assembly, the strain gages were mounted at the center on both the tension and compression faces of the tube while in the case of the four-layered tube assembly, both the strain gages were attached to the tension face of the structure. The center of the compression face of the four-layered sample was used for loading and so no strain gage could be mounted on it.

2.3 TEST PROCEDURE

The loading of the single tube was done in cycles of 6.68 kN (1,500 lb). For the double tube the loading cycle was increased to 13.35 kN (3,000 lb) while for the four-layered tube assembly the loading cycle was 22.25 kN (5,000 lb). The cyclic loading of the specimen was done so as to evaluate damage accumulation, stability and any residual deflection, strain or any energy loss occurring in it due to the applied load. Significant events such as cracking sounds, distortion of the shape of the tubes and breaking of the joints or fibers were observed whenever possible. The load was gradually increased and the rate of loading and unloading was kept constant during all the tests. Data sampling frequency was sufficiently high to capture all the important events in the course of the test.

All the three specimens were tested to failure. The single tube took a load of 24.12 kN (5,420 lb), the double tube assembly took 62.30 kN (14,000 lb) while the four-layered tube assembly took a load of 182.76 kN (41,070 lb) before failure.

2.4 FAILURE MODE

Static tests were conducted on the samples to determine ultimate static strength and failure progression. All the tests conducted were load controlled. Composite materials exhibit very complex failure mechanisms under static loading because of their anisotropic nature. Failure may involve multiple damage modes that can be observed as fiber breakage, matrix cracking, interfacial debonding, delamination, or a combination of these failures. The ultimate bending strength of pultruded composite beams is limited by various failure mechanisms. Local buckling of the thin walls precipitates most failure modes. It initiates a failure mode that eventually results in material degradation and total failure of the beam.

In the case of single tube and double tube assembly, the loading was done in cycles as previously specified until the point of failure. The failure occurred at one of the points of loading and distinct cracks appeared on the top surface and sides of the tubes. The regions of failure of a single tube, double tube and four-layered tube assembly are shown in Figures 2, 3 and 4 respectively. In both the cases, the local buckling of the compression flange initiated the failure resulting in the failure of the sample. Cracks developed at the web-flange junction due to buckling leading to the separation of web and flange. This was followed by the bending of the web about its weak axis developing cracks at the middle of the web. A delamination crack of the compression flange was

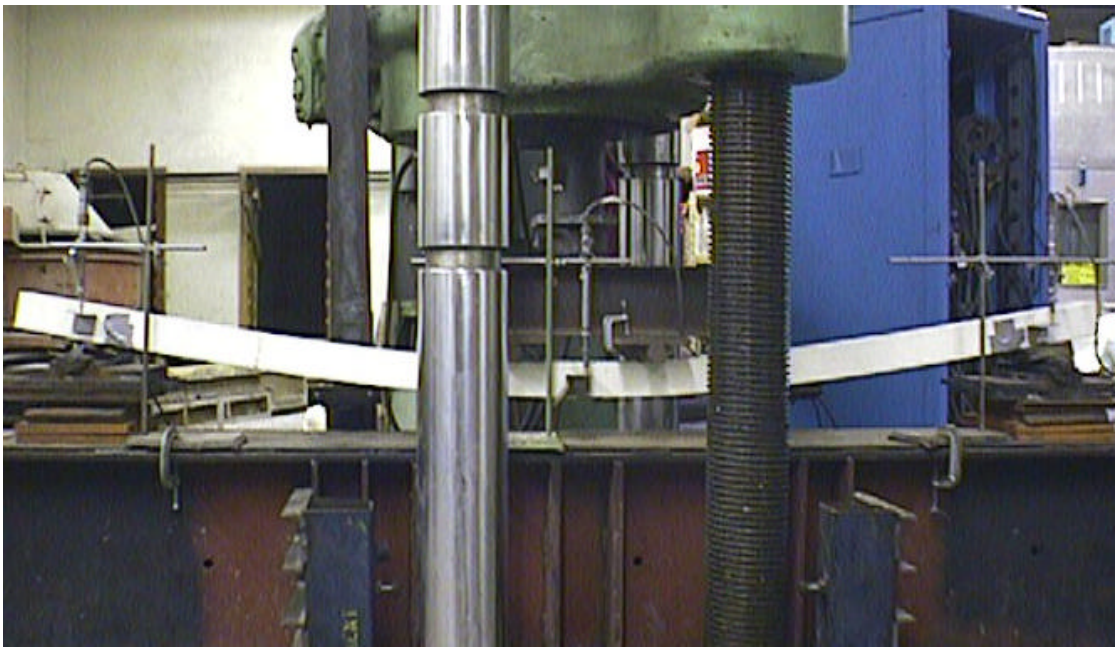

(a)

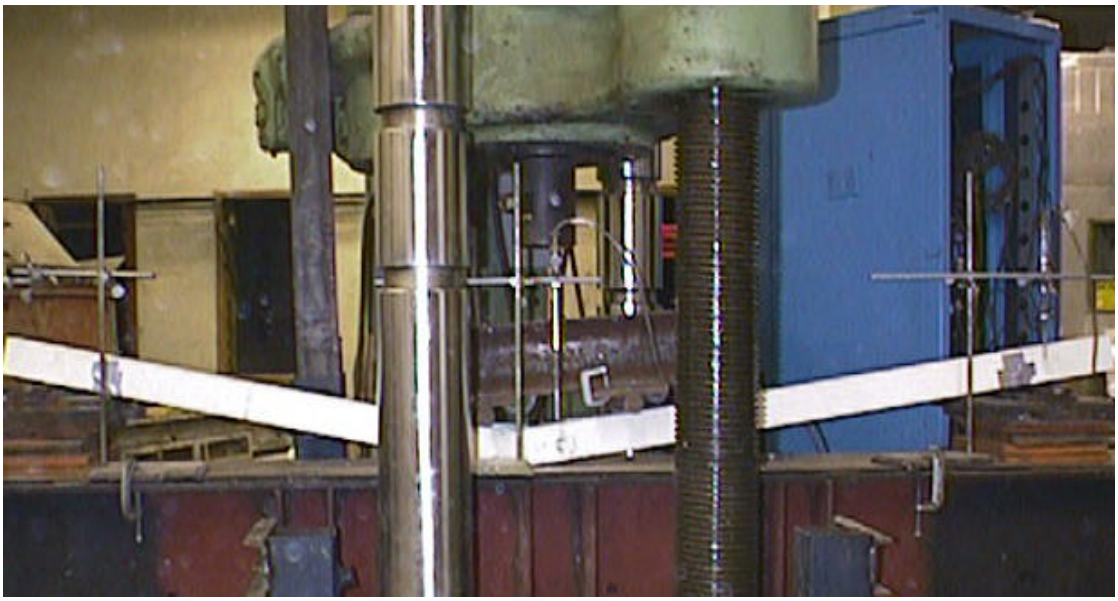

(b)

Figure 2: A single GFRP tube immediately (a) before and (b) after failure.

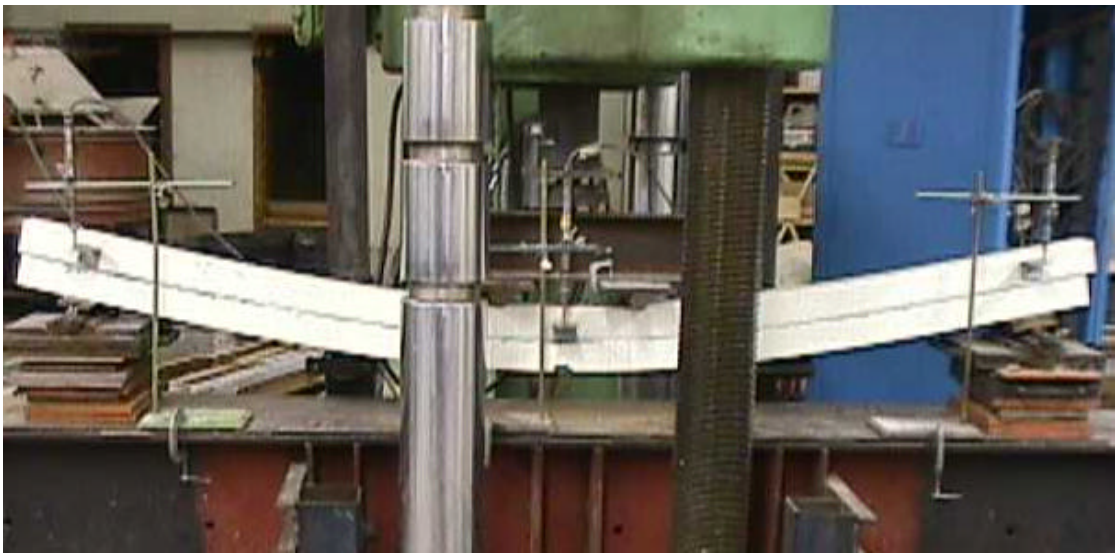

(a)

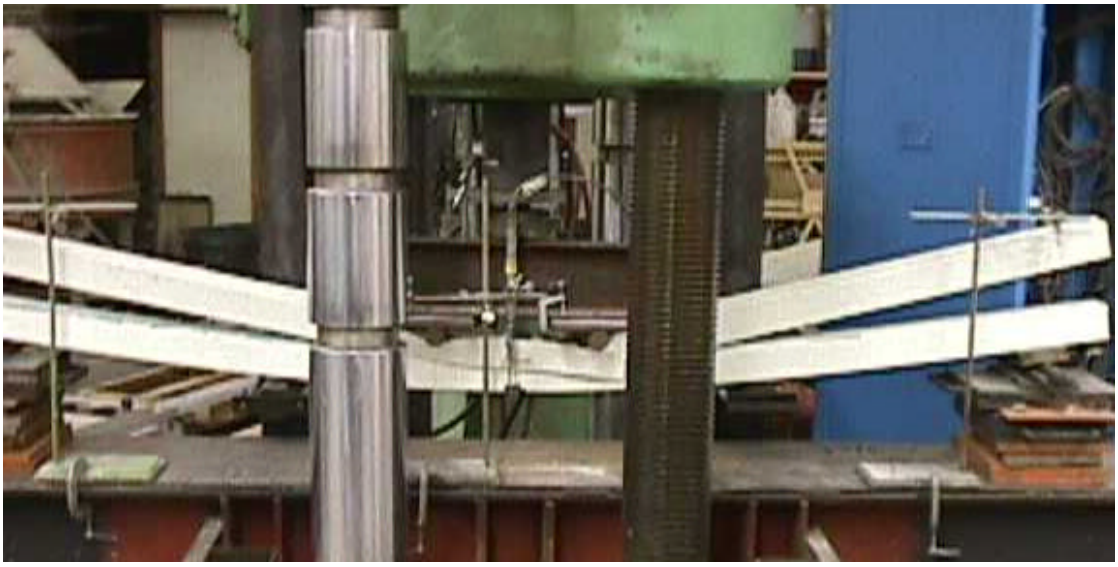

(b)

Figure 3: A double GFRP tube assembly immediately (a) before and (b) after failure.

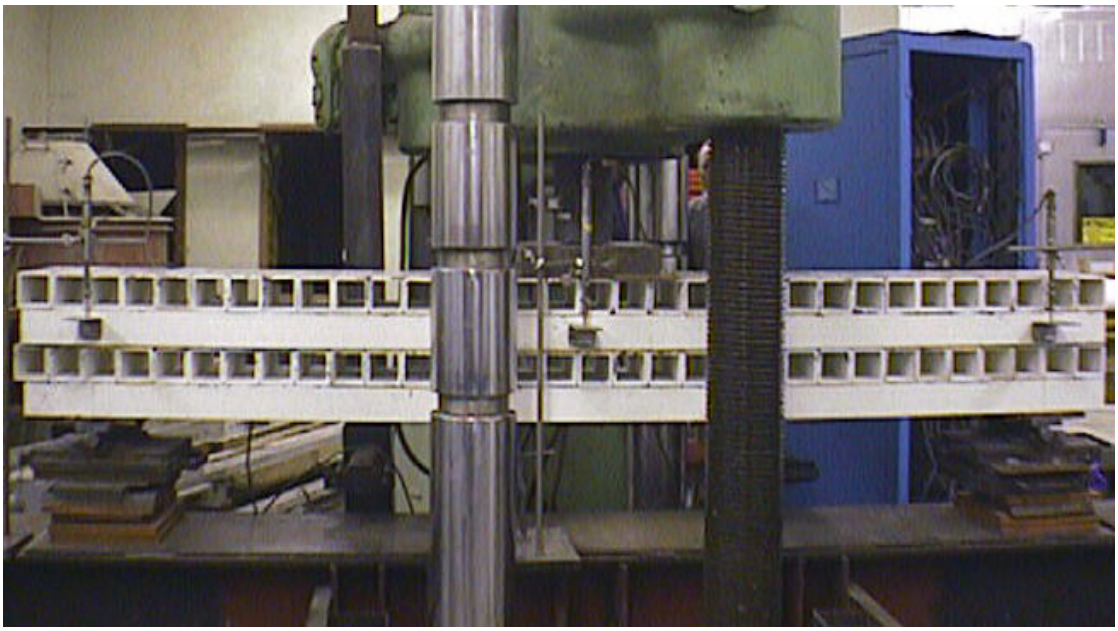

(a)

(b)

Figure 4: A four-layered GFRP tube assembly under loading (a) experimental set-up and (b) deflection under loading.

observed. The flange cracks then propagated into the web leading to the final failure of the section.

The failure mode of the four-layered tube assembly was very different than those of the other two samples. As the load was applied, this structure exhibited progressive damage accumulation with the increase in load, indicated by the cracking sounds observed. The first few cracking sounds started at about 89 kN (20,000 lb). The origin of the sound could not be determined. However, based on the observed ultimate load, the most likely cause of the sounds was breaking of the adhesive bonding between the tubes of the assembly. The micro fracture continued to occur with increasing loads, however, they were reduced, or did not continue during cyclic loading, indicating stability. At about 111.25 kN (25,000 lb) some deformations in the shape of the tubes of the first and third layers were observed. The tubes in these layers were acted upon by compressive force due to the loading. These tubes, laid down transversely to the direction of traffic, started to bend away from the center changing their shape from square to a parallelogram. As the load was increased to 133.50 kN (30,000 lb), cracks appeared along the corners of few of the tubes in the first and third layers due to the twisting motion. Breaking of fibers and delamination was also was observed in these layers. The noise coming from the sample had increased considerably. At a load of 182.76 kN (41,070 lb), a few of the small tubes from the first layer popped out of the structure due to the compressive load on them. It was observed that several tubes in the first and the third layers had cracked and had been bent away from the center towards one of the sides. No damage was observed in the second and fourth layers, which were the main load bearing members. The mode

of failure observed was transverse shear failure resulting in the delaminations and cracking of fibers along the edges of the GFRP pultruded tubes. Figures 5 and 6 show the regions of failure for a single tube and double tube, respectively. Figure 7 shows the bending and distortion of the GFRP tubes under bending and also the sample after failure due to the popping out of tubes from the top layer.

(a)

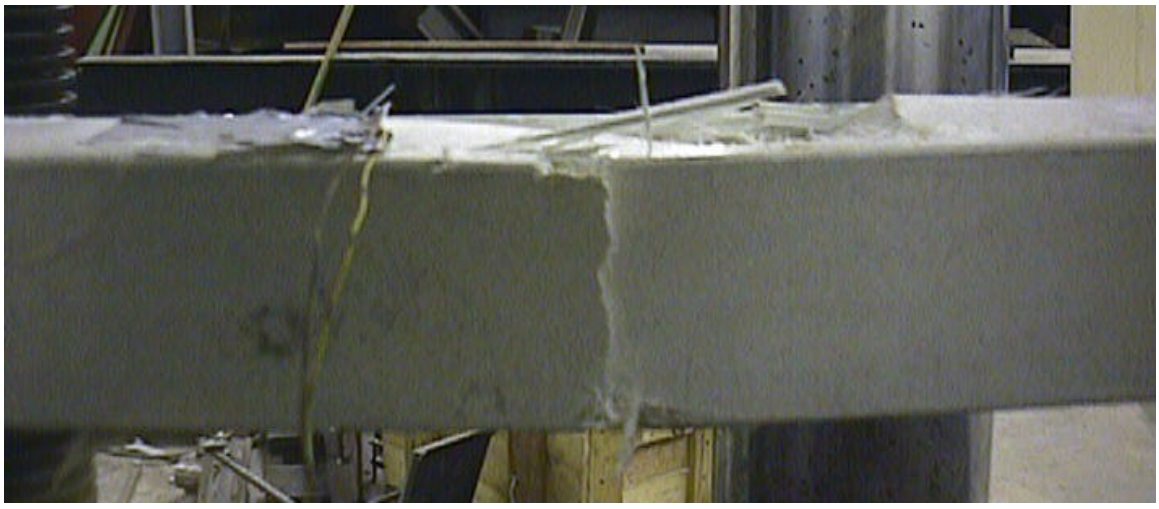

Figure 5: The regions of failure of a single GFRP tube on (a) the top surface and (b) the sides.

(a)

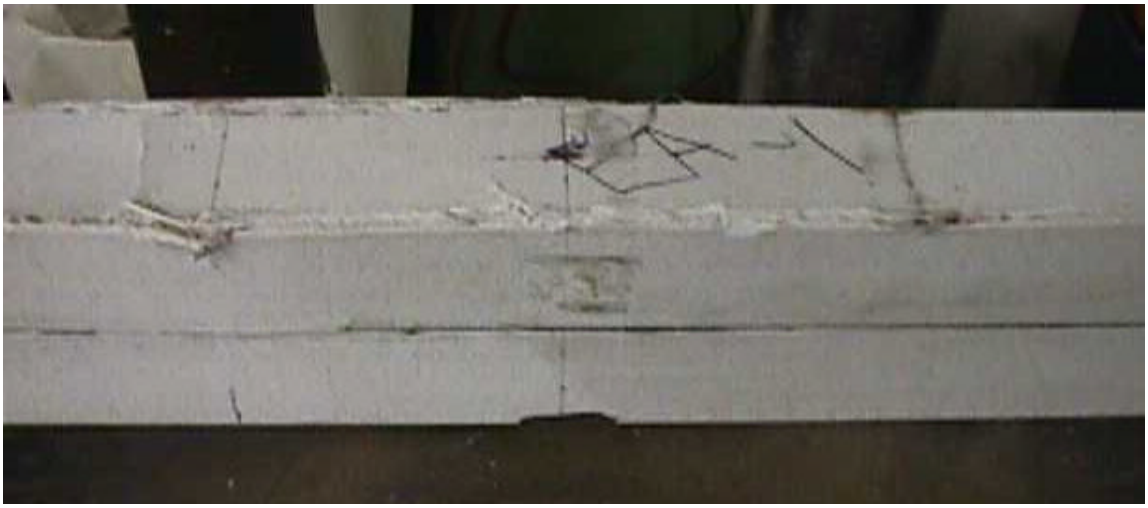

(b)

Figure 6: The regions of failure of the double tube assembly on (a) the top surface and (b) the sides

(a)

(b)

Figure 7: Four-layered tube assembly (a) under bending, showing distortion of the GFRP tubes, and (b) after failure.

2.5 TEST RESULTS

The test results are presented separately for deflection and strain. Key information is presented and discussed in the following sections. In general, data for all three samples have been presented together for each type of measurements as opposed to showing all the data for each one of them in succession.

2.5.1 DEFLECTION

The load-deflection plots for the three specimens show the complete curves, and indicate gradual stiffness degradation with increasing load levels. In the case of single tube and double tube assembly, the observed behavior is essentially linear elastic up to failure. In the case of the four-layered tube assembly, it shows a linear elastic behavior up to a load of about 89 kN (20,000 lb) beyond which the structure exhibits distinct non-linear characteristics. The failure of the single GFRP tube occurred at a load of 24.12 kN (5,420 lb) and the total deflection of the tube at this point was 139 mm (5.47 in). Figure 8 (a) shows the graph of deflection plotted against the applied load for the single tube test. The double tube assembly took a load of 62.30 kN (14,000 lb) and had a maximum deflection of 63.3 mm (2.49 in). Figure 9 (a) shows the graph of deflection plotted against applied load for this specimen. The maximum load taken by the four-layered tube before failure was 182.45 kN (41,000 lb). The deflection at this load was 81.3 mm (3.2 in). Because the assembly can show non-linear characteristics beyond 89 kN (20,000 lb), only the data up to this load is taken into consideration. Figure 10 (a) shows the graph of deflection plotted against the applied load in the elastic region for this specimen. The stiffness degradation of the three specimens with increasing load appears to be

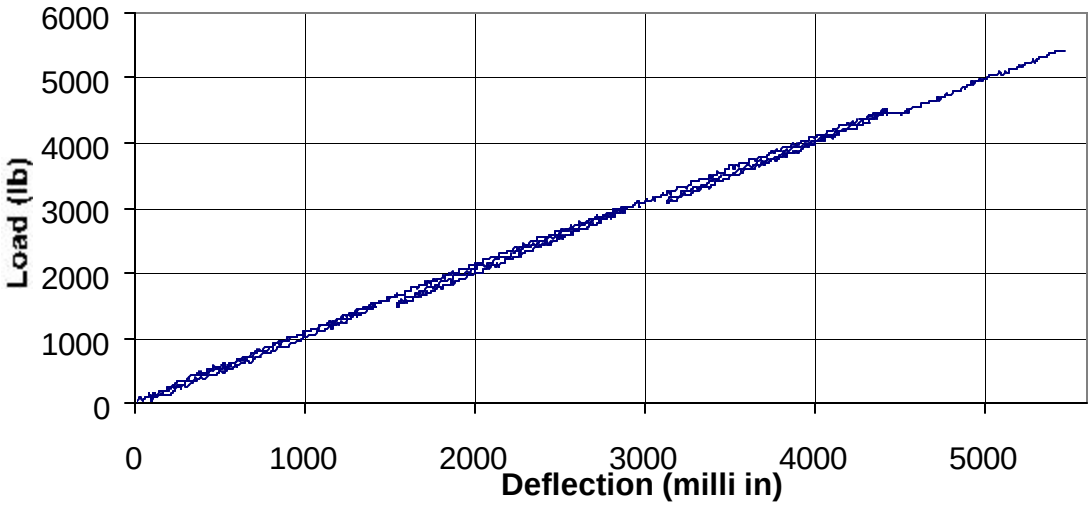

(a) Load Vs. Deflection

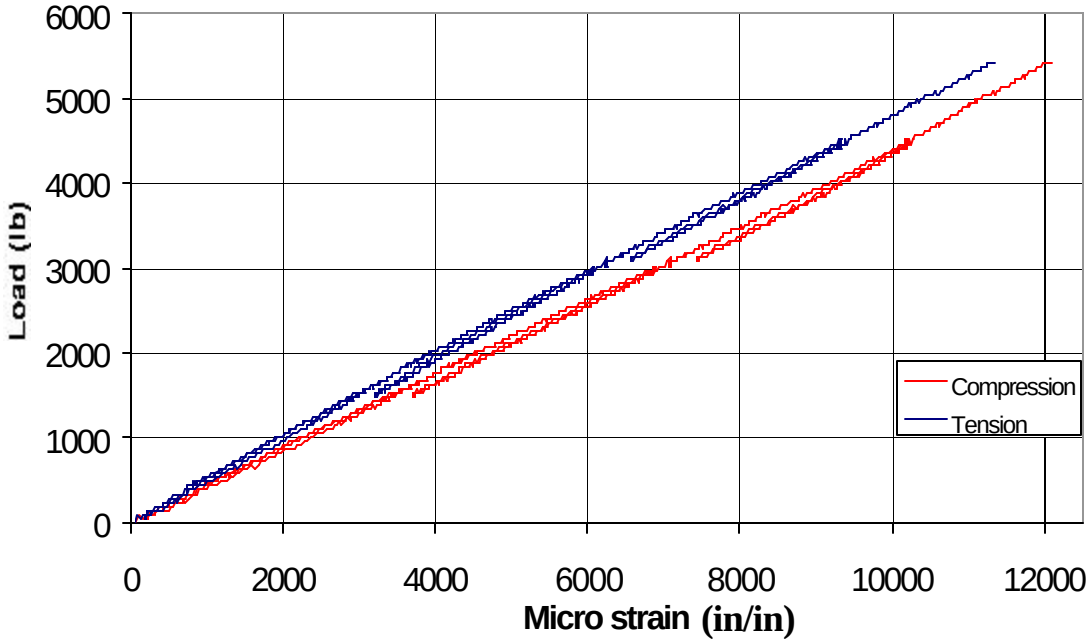

(b) Load Vs. Strain

Note: 1 in = 25.4 mm, 1 lb = 4.45 N

Figure 8: Graphs of (a) deflection and (b) strain in a single GFRP tube test plotted against applied load.

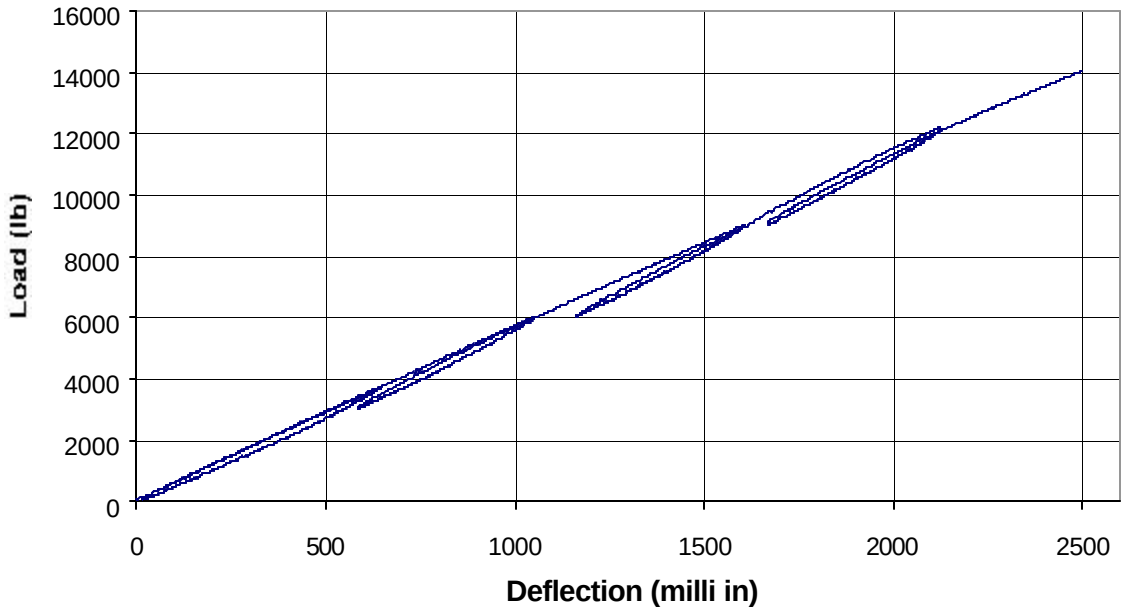

(a) Load Vs. Deflection

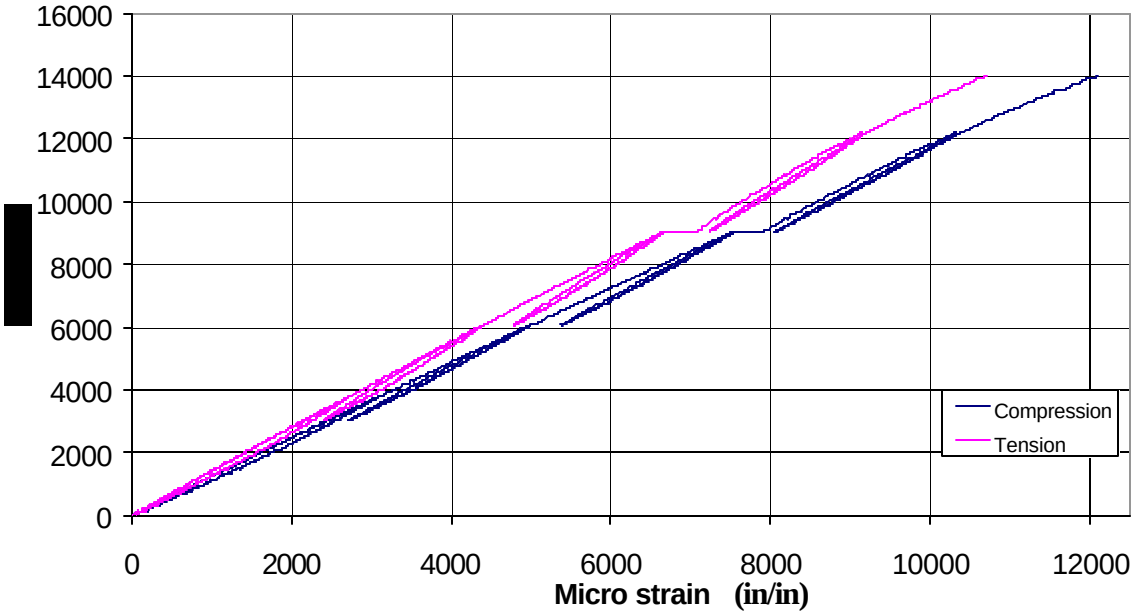

(b) Load Vs. Strain

Note: 1 in = 25.4 mm, 1 lb = 4.45 N

Figure 9: Graphs of (a) deflection and (b) strain in a double tube assembly test plotted against applied load.

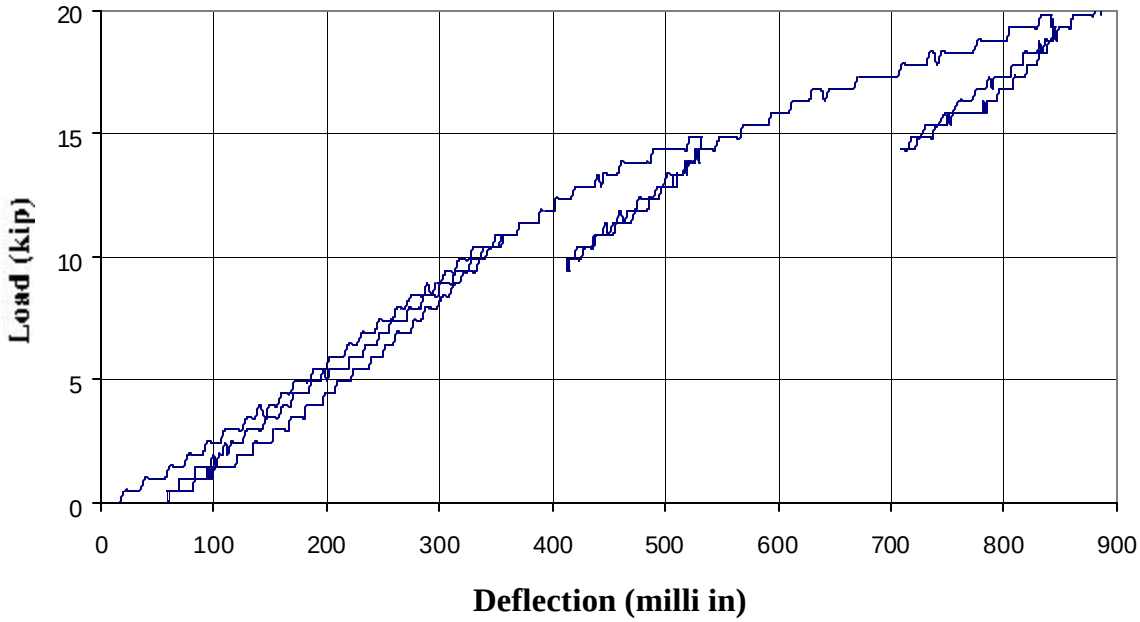

(a) Load Vs. Deflection

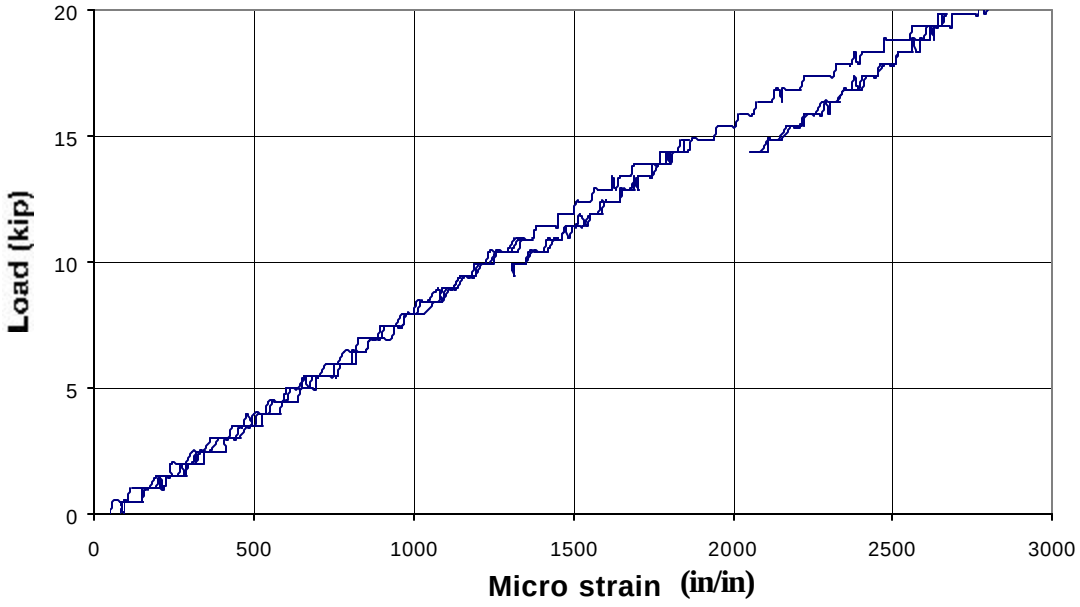

(b) Load Vs. Strain

Note: 1 in = 25.4 mm; 1 kip = 4.45 kN

Figure 10: Graphs of (a) deflection and (b) strain in a four-layered tube assembly test plotted against applied load.

caused by damage accumulation, which is indicated by the small load drop in the loading curves.

2.5.2 STRAIN

Two strain gages were attached to each of the specimens to measure the surface strains developed. In the case of single tube and double tube assembly, the strain gages are connected to the center of the top and bottom surfaces to measure the compressive and tensile strains. In the case of four-layered tube assembly both the strain gages were connected at the bottom of the structure as the center of the compressive face was used for loading. Figures 8 (b), 9 (b) and 10 (b) show the graphs of strain plotted against the applied load in the case of a single tube, double tube and four-layered tube assembly respectively. The graph for the four-layered tube assembly is shown only up to the linear elastic region. In general the strain results are excellent and indicate good symmetry about the centerline.

The data obtained from the deflection and strain reading for the single tube and double tube assembly were used for calculating the flexural rigidity or Young's modulus, E, of the tube. In the case of a single tube, the Young's modulus obtained using deflection criteria was 24.27 GPa (3,520 ksi), using compressive strain its value was 22.96 GPa (3,330 ksi), while tensile strain gave a value of 26.13 GPa (3,790 ksi). For the double tube assembly, the Young's modulus obtained using deflection criteria was 24.13 GPa (3,500 ksi), using compressive strain its value was 22.48 GPa (3,260 ksi) and that obtained using tensile strain was 25.37 GPa (3,680 ksi). The experimental results showed that the composite beams can experience large deformations and strains with the material remaining in the linear region. In the case of the double tube assembly it also showed that the assembly behaves as a single unit and that the bonding between the two tubes

was perfect. Investigation of the bending behavior of GFRP tubes shows that the bending stiffness is low compared to that of steel sections of the same shape. It also indicates that shear deformation effects are significant. This is a consequence of the relatively low modulus of elasticity of the glass fibers, as compared to steel, and the low shear modulus of the resin. Most significantly, due to the large elongation to failure allowed by both the fibers (4.0%) and the resin (4.5%), the composite material remains linearly elastic for large deflections and strains (Fu et al. (1990). As a consequence of local buckling, large strains are induced during post-buckling. These large strains ultimately lead to the failure of the material and subsequent total failure of the member.

3. STRUCTURAL PERFORMANCE OF A FRP BRIDGE DECK

3.1 BRIDGE DECK DESIGN

The development of a sound composite bridge deck requires consideration of the special needs of composite structural design, as well as the application of standard civil engineering practice and validation to ensure public safety. This dictates the requirement for significant amounts of material testing and experimental validation as existing design techniques for composite structures are applied to bridge applications.

3.1.1 DESIGN PARAMETERS

This bridge deck was designed to AASHTO specifications for a 9.14 m (30 ft) span vehicular traffic bridge using the load configuration shown in Figure 11. AASHTO bridge design specifications limit the deflection of the deck to 1/800 of the span length, L, of the bridge deck. According to the specifications, the flexural members of the bridge structures should be designed to have adequate stiffness to limit deflections or any deformations that may adversely affect the strength or serviceability of the structure.

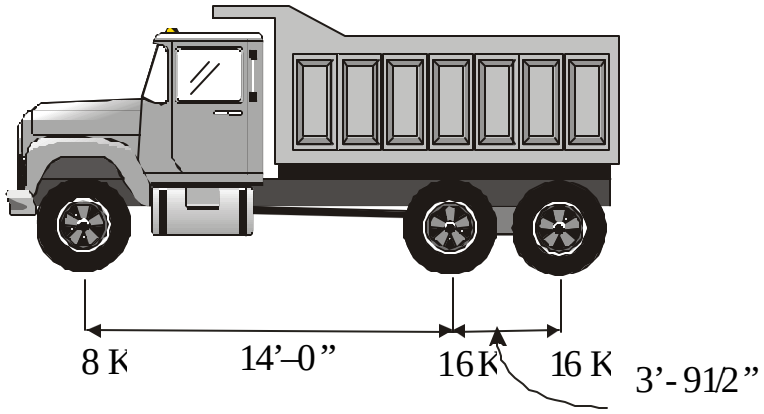

Figure 11: H-20 Truck
Note: 1 ft = 12 in = 304.8 mm; 1 kip = 4.45 kN

3.1.2 DESIGN OF BRIDGE DECK AND TEST SAMPLE

The bridge deck was fabricated using varying lengths of pultruded hollow tubes composed of glass and carbon fibers in vinyl ester matrix. The tubes have a square cross-section of 76 mm (3 in) and a thickness of 6.4 mm (0.25 in). Extensive analysis and testing of single, double and four-layered GFRP tube assemblies were conducted to evaluate the characteristics of the tubes. The static behavior of single GFRP tubes were analyzed under flexure followed by testing of double tube assemblies and a four-layered tube assembly. The double tube assemblies were prepared using three different epoxy adhesives and tested to failure under flexure. The results of the tests aided in the selection of the adhesive to be used for almost perfect bonding between the tubes and also provided knowledge about the behavior of the tubes in an assembly. Finally, a four-layered tube assembly was tested to failure under flexure. The deflection, strain and failure modes of the various test coupons were analyzed. The stiffness of the tubes and their assemblies demonstrated that they could be used in the building of all composite bridge decks and for other infrastructure applications.

Analysis of the bridge deck design using FEA led to an I-beam structure made up of eight layers with alternate layers of tubes laid down transversely and longitudinally to the direction of the traffic. These tubes were adhered to each other using an epoxy adhesive and were further mechanically fastened together using screws. All mated surfaces were abraded before applying the epoxy adhesives, and pressure was applied on them until curing was complete. The design of the bridge deck consisted of four identical I-beams running along the length of the deck. In the present work the layers of tubes have been numbered from the top to the bottom of the deck with the topmost layer being

the first layer and the bottom layer of tubes being the eighth layer of the deck. The second and eighth layers consisted of 9.14 m (30 ft) long carbon fiber-reinforced polymer (CFRP) tubes that were used to impart stiffness to the structure. The remaining six layers were made up of GFRP tubes. The first, third and seventh layers were built using 2.74 m (9 ft) long tubes. The fourth, fifth and sixth layers of tubes formed the neck or web of the I-beams. The fourth and sixth layers were assembled using 9.14 m (30 ft) long tubes while the fifth layer, the center layer in the neck of the I-beam, was made up of 305 mm (1 ft) long tubes. The second, fourth, sixth and eighth layers were laid down parallel to the direction of the traffic and were the main load bearing members of the structure. The first, third, fifth and seventh layers were laid down transverse to the direction of traffic. These layers had very limited load carrying capacity and were used mainly to transmit load to the lower lying load carrying layers.

The prototype deck sample built for conducting the fatigue and failure tests had the same number of layers of tubes laid down in a similar pattern as the bridge deck. The test sample had dimensions of 9.14 m (30 ft) long by 610 mm (2 ft) wide by 610 mm (2 ft) high. It was equivalent to a quarter of the bridge deck and had the cross-section of a single I-beam. After results of the tests conducted on the prototype deck sample were analyzed, it was observed that the performance of the sample exceeded the design specifications. Consequently, one of the layers of GFRP tubes was deemed unnecessary. It was decided to eliminate the topmost layer of GFRP tubes from the original design while still meeting all the design criteria. This leads to reduction of cost, thickness and weight of the structure, as compared to the original design. Thus the final design of the bridge deck consisted of seven layers of tubes with the CFRP tubes forming the first and

last layers of the deck. The final dimensions of the bridge deck were 9.14 m (30 ft) long by 2.74 m (9 ft) wide by 533 mm (21 in) high. A thin polymer concrete wearing surface or overlay was added to the top of the full-size bridge deck. This polymer concrete overlay was required to have high tensile elongation due to the flexible response of the FRP composite deck. It was also needed to develop good adhesion to the GFRP deck surface, provide a non-skid surface, absorb energy and should be easy to place on the deck surface. Upon evaluating the results of studies done by a few authors (Lopez-Anido et al. (1998a)) in polymer concrete, it was decided to use Transpo T48, an epoxy based system used on several FRP bridges, along with an aggregate of tan Trowlrite. The aggregate was applied by hand after the epoxy layer was spread across the bridge. The thickness of the wearing surface was roughly 6.4 mm (0.25 in). However, for the prototype deck sample, the wearing surface was not included as it was assumed that it would not significantly affect the structural response of the deck panel. The cross-sectional geometry and overall dimensions of the bridge deck and the test sample are shown in Figures 12 and 13 respectively.

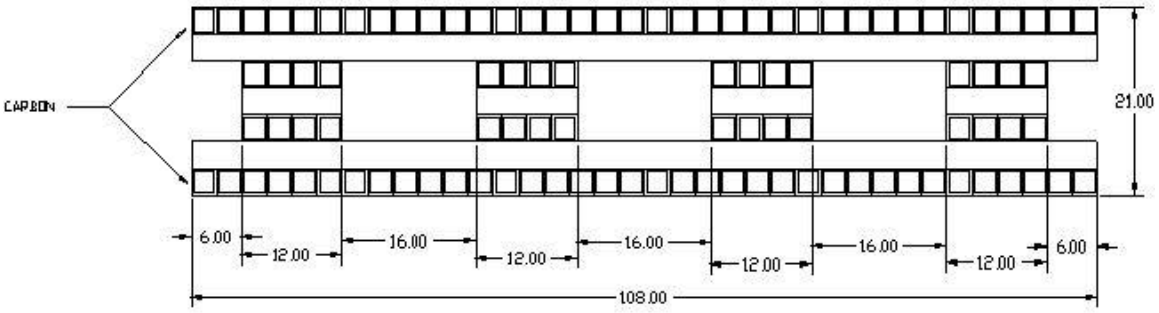

(a) Schematic diagram of the full-size bridge deck showing the side view and the dimensions

Note: All dimensions are in inches; 1 ft = 12 in = 304.8 mm

(b) Longitudinal cross-section of full-size bridge deck

Figure 12: Diagram showing (a) overall dimensions and (b) actual longitudinal cross-section geometry of the full-size bridge deck

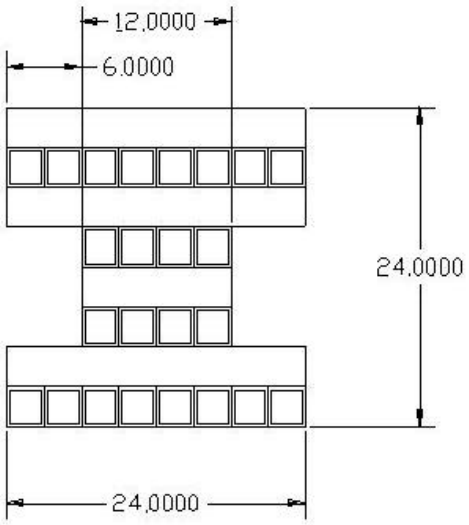

(a) Schematic diagram of the bridge deck test sample showing side view and the dimensions

Note: All dimensions are in inches; 1 ft = 12 in = 304.8 mm

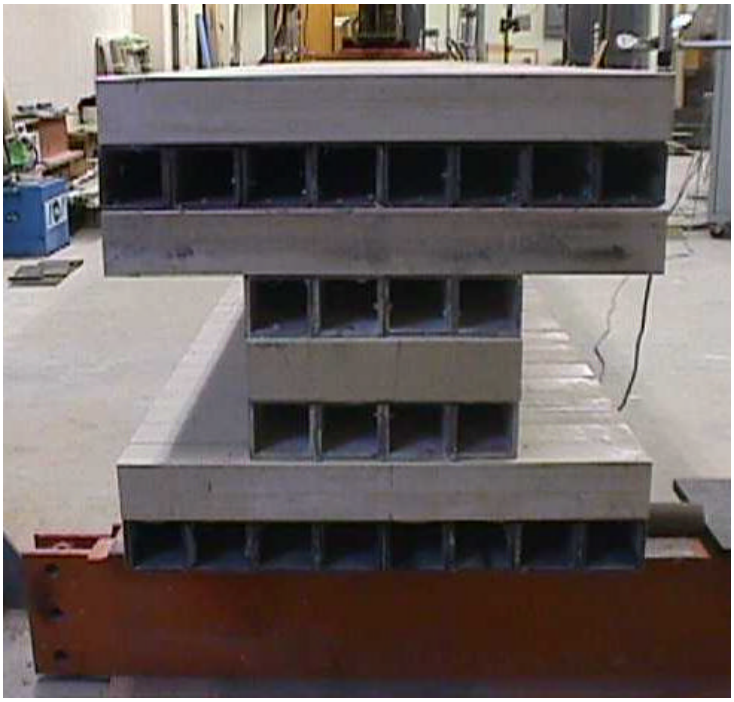

(b) Longitudinal cross-section of bridge deck test sample

Figure 13: Diagram showing (a) overall dimensions and (b) actual longitudinal cross-section geometry of the bridge deck test sample

3.2 TEST PROGRAM

The overall philosophy of the composite deck test program was to determine characteristics of the full-size bridge deck by analyzing the tests performed on relatively smaller sections of same design. The design and dimensions of the prototype deck sample used for testing has been discussed in the previous section. The objectives of testing the sample were threefold: (1) to investigate feasibility of the proposed configuration and to verify that the composite bridge meets all the design requirements specified by AASHTO for a 9.14 m (30 ft) long bridge deck with an H-20 truckload; (2) to investigate the local stresses and strains developed at the points of load application and supports; (3) to provide the ground work for analyzing characteristics of the full-size bridge deck. The results of the study on a quarter portion of the bridge deck can reasonably be extrapolated to the full-size bridge deck. Three different tests were performed on the deck sample for obtaining all the useful design performance information and to study its structural behavior. Specifically, the following tests were performed: (1) design load test (quasi-static loading up to the design load in the mid-span of the deck); (2) fatigue or cyclic load test (fatigue loading under service loads to 2 million cycles with quasi-static load tests at periodic intervals to assess degradation); (3) ultimate load test (static loading to failure with load at mid-span of the deck).

3.2.1 EXPERIMENTAL SETUP AND INSTRUMENTATION

The composite deck test sample was simply supported at the ends using two rollers spaced at a distance of 8.54 m (28 ft) so that the beam extended 305 mm (1 ft) beyond the support rollers at each end. The rollers were 610 mm (2 ft) long and were supported in between rails resting on the floor. In case of the static load tests, namely the design load test and the ultimate load test, a temporary setup was put up on the floor.

Load was applied using a 889.6 kN (200,000 lb) manual hydraulic jack aligned to the center of the deck and overhanging from four screws fixed vertically to the floor. A manually controlled hydraulic pump was used to load and unload the jack. Figure 14 shows the experimental setup of the bridge deck test sample for the static tests. In the fatigue test load was applied using a MTS electro-hydraulic actuator permanently fixed to a framework. The actuator had a loading capacity of 97.9 kN (22,000 lb) and a stroke of 152.4 mm (6 in). This test was controlled using a MTS 436 controller. Test setup for the fatigue load test is shown in Figure 15. A 1.52 m (5 ft) long spreader beam was utilized to apply the load at mid-span. This spreader beam was supported by the deck sample via two stacks of 101.6 mm (4 in) thick steel plates used as loading patches. These rectangular loading patches of 203 mm (8 in) by 508 mm (20 in), with the larger dimension transverse to the direction of traffic, were used to simulate the action of wheel loads of an H-20 truck on top surface of the deck. The loading patches were at a distance of 1.22 m (4 ft) or 610 mm (2 ft) off-center, representative of the distance between the two back axles of an H-20 truck. This setup leads to a four-point bending load configuration as shown in the schematic diagram in Figure 16.

Figure 14: Experimental setup for the four-point static tests on the bridge deck test sample

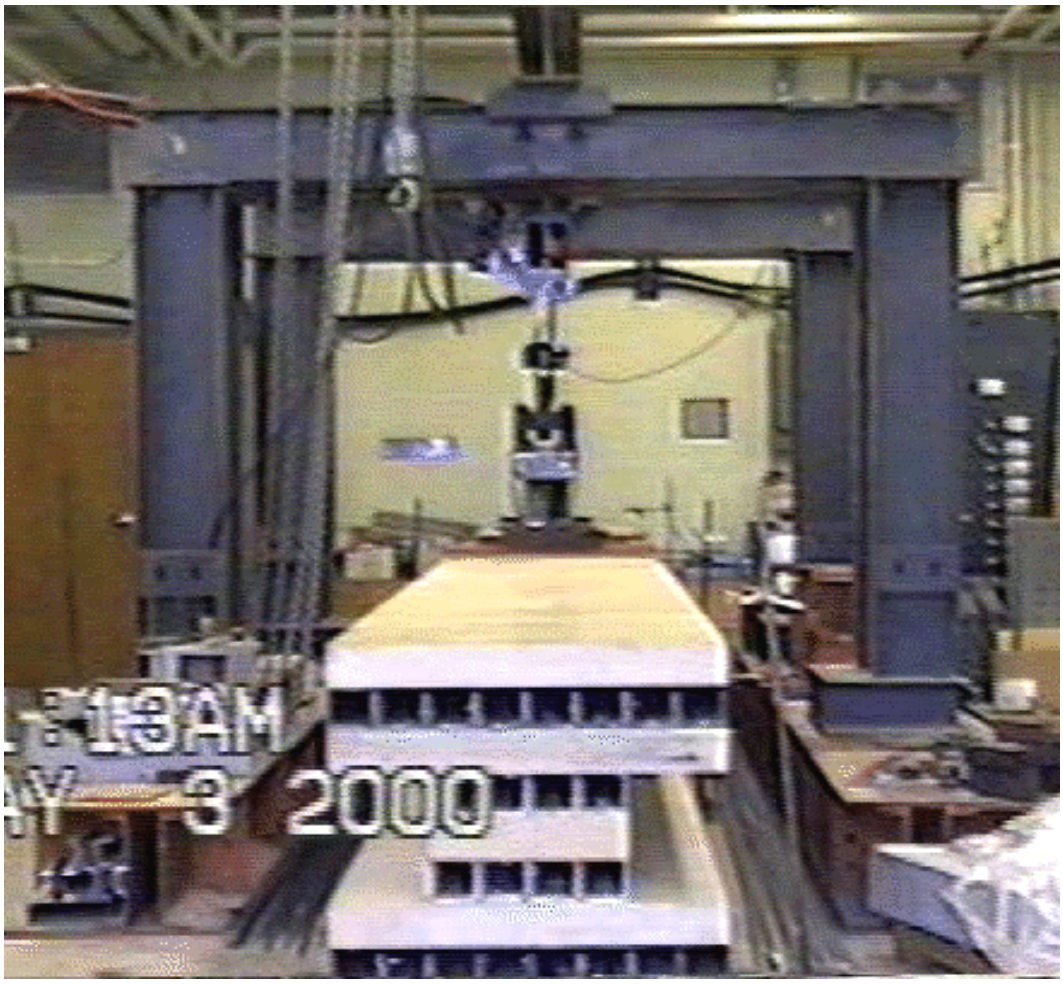

Figure 15: Experimental setup for the fatigue load tests

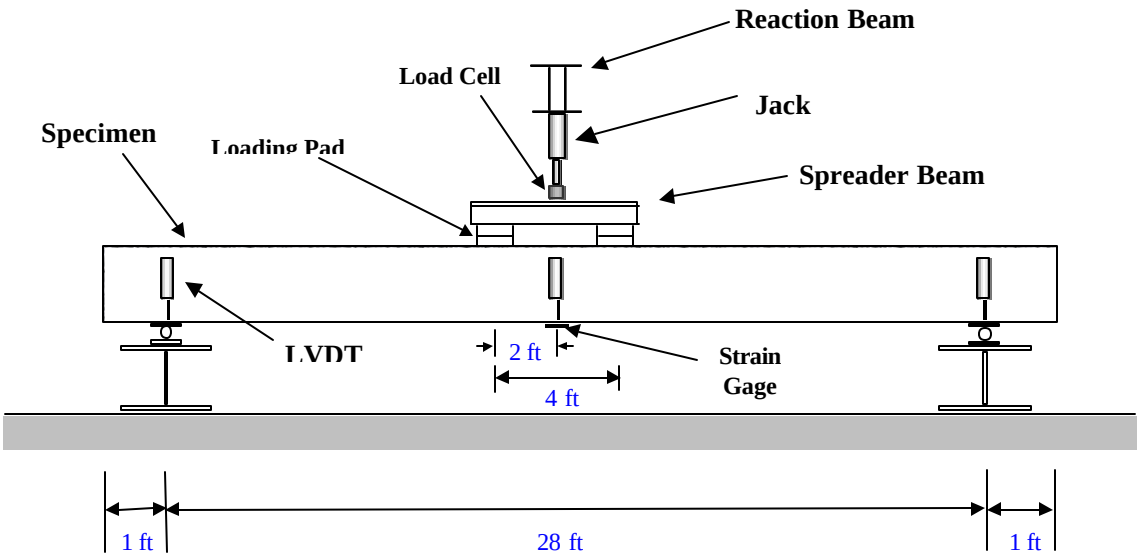

Figure 16: Schematic of four-point bend geometry
Note: 1 ft = 12 in = 304.8 mm

Variations of deflection and strain measurements with number of cycles and mode of failure after loading cycles were used to characterize the fatigue and strength performance of the bridge deck. LVDTs (Linear variable differential transformers) were installed at mid-span and at the two supports to measure deflections of the deck. The LVDT at the center had a stroke length of 50.8 mm (2 in) while those at the supports had a stroke length of 25.4 mm (1 in). Ten 6 mm (0.24 in) long 120 ohms electrical resistance strain gauges were attached to the tubes of the bridge deck at several important locations to obtain the strain readings. Longitudinal and transverse strains were measured on the top and bottom deck surface at the center of the deck. Strain gauges were also attached to other pertinent locations on different layers of FRP tubes. The locations of LVDTs and one of the strain gauges at the bottom face of the test sample are shown in Figure 16. The vertical load applied on to the test sample was measured using a 222 kN (50,000 lb) load cell placed between the hydraulic jack and the spreader beam. In case of the fatigue test, a 97.9 kN (22,000 lb) load cell was used which was a part of the MTS hydraulic actuator loading system. A MTS 436 controller was used to control the load range, frequency of loading and the number of cycles of the hydraulic actuator. Load, deflection, and strain signals were continuously recorded during testing using a high-speed data acquisition system.

3.3 EXPERIMENTAL PROCEDURE AND RESULTS

Three different tests were conducted on the prototype deck sample. Each of these have been discussed separately.

3.3.1 DESIGN LOAD TEST

This was a preliminary test for observing behavior, assessing serviceability and performance of the composite bridge deck up to a load of 111 kN (25,000 lb). It also helped to investigate feasibility of the proposed configuration and to verify that the composite bridge meets all AASHTO design requirements for an H-20 truckload. The design load for quarter portion of the bridge deck was 94.8 kN (21,320 lb). The load of 111 kN (25,000 lb), being slightly higher than the design load, was chosen as the higher limit for this test. The deck sample was tested under flexure in four-point loading configuration at the mid-span. The deflection of the deck was 22 mm (0.86 in) at the highest load limit and only a very slight bending of the deck could be observed by visible inspection. As the load was increased beyond 80 kN (18,000 lb), a few cracking sounds were heard which appeared to be cracking of the adhesive layer in between a few of the tubes. Figures 17 and 18 show the plots for load versus deflection and strain for the design load test respectively. The plots show that the deflection and strain behavior were linear elastic throughout the test. The results were extremely encouraging as the deflection of the test sample was only 6.6 mm (0.26 in) upon application of a quarter of the design load 35.5 kN (8,000 lb). The deck does not show any premature deterioration or damage at this load.

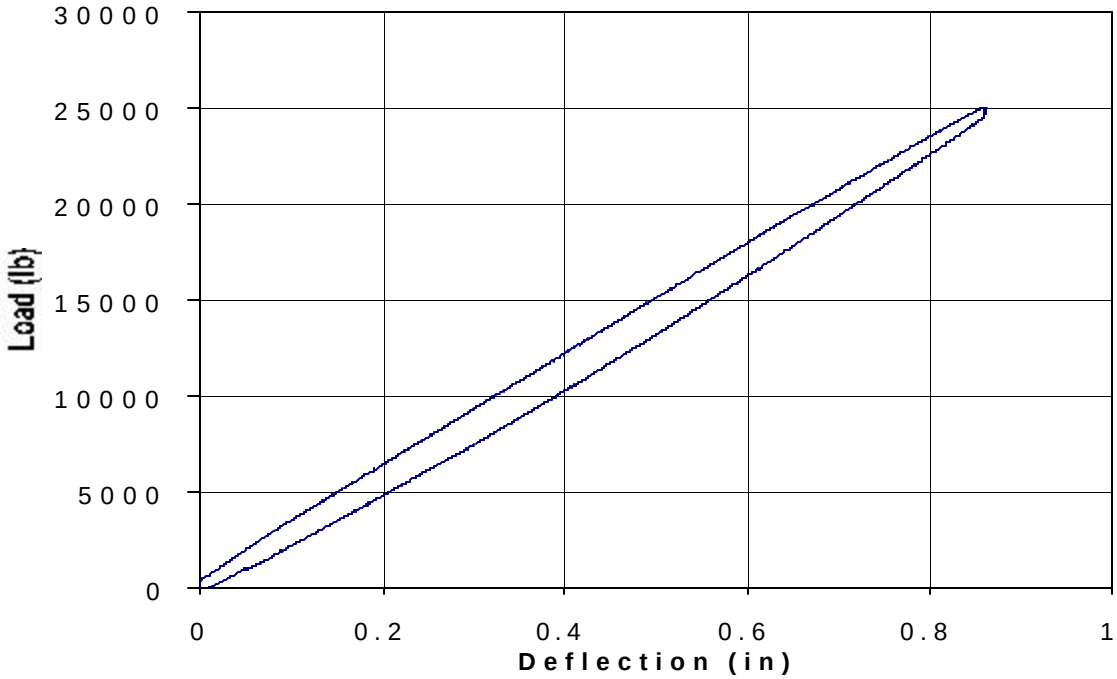

Figure 17: Load-deflection curve for design load test up to a load of 111 kN (25,000 lb)

Note: 1 in = 25.4 mm, 1 lb = 4.45 N

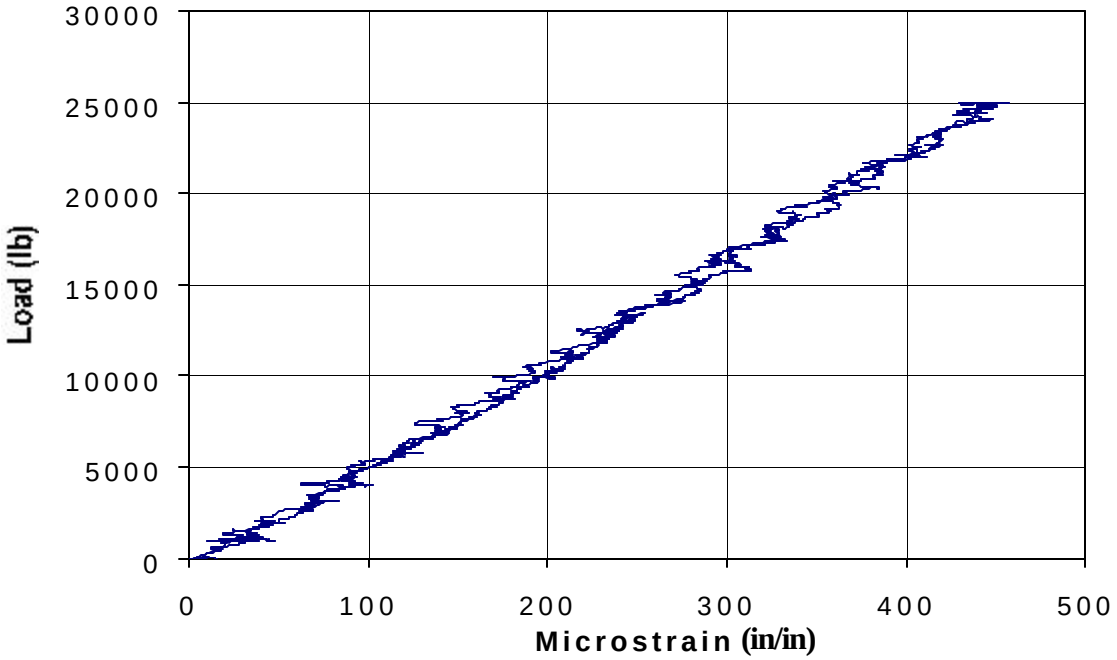

Figure 18: Load-strain curve for design load test up to a load of 111 kN (25,000 lb)

Note: 1 in = 25.4 mm, 1 lb = 4.45 N

3.3.2 FATIGUE OR CYCLIC LOAD TEST

The second test performed on the deck sample was a fatigue or cyclic load test, the setup for which has been described in previous sections. Fatigue is an important issue where the load on a structure is almost entirely transient. Normally, tests are run for no more than 2 to 3 million cycles, even though, for many infrastructure applications, this may represent only a few years of actual service. Sometimes, an attempt is made by researchers to "accelerate" the fatigue damage by testing at loads much higher than the service load. However, this approach is inadequate as different damage mechanisms may dominate under different load levels. Taking this into consideration, this deck sample was subjected to fatigue loading for 2 million cycles at a minimum/maximum load ratio of R=0.045 with the maximum load of 48.93 kN (11,000 lb) and the minimum of 2.2 kN (500 lb). The maximum load was slightly higher than the service load of 48.1 kN (10,800 lb) for the deck sample. The loading cycles simulate passage of the back axles of an H-20 truck over the points of application for that many number of cycles. Before starting the fatigue test, a quasi-static flexure test up to a load of 88.96 kN (20,000 lb) was performed. A similar quasi-static test was performed after every 400,000 cycles. The static load tests served as a periodic measure of potential changes in the stiffness of the structure due to the live load induced degradation. It also helped to periodically inspect signs of deterioration, if any, of the deck sample caused by the fatigue loading.

The fatigue test was conducted under load control condition with the maximum and minimum load kept constant at a frequency of 4 Hz. A total of six quasi-static flexure tests were conducted on the sample during the course of this test after 0, 0.4, 0.8, 1.2, 1.6 and 2 million cycles. Figures 19 and 20 show comparison of the results from

deflection and strain measurements against the load applied during the static tests respectively. The plots show that the deck deflection and strain responses remained fairly constant for all the static load tests and no apparent loss in stiffness was demonstrated up to the maximum applied load of 88.96 kN (20,000 lb). A thorough visual inspection of the test sample was done at the time of each static load test and no sign of fracture or debonding between the FRP tubes in any of the eight layers, due to the fatigue loading, was observed. The fasteners holding on to the tubes, in addition to the adhesive, were also inspected and were found to be in perfect condition. The height of the test sample from the floor was recorded before starting a new set of 400,000 cycles and after its completion. On comparison it revealed that no permanent bending of the deck sample had taken place. No other form of damage was observed either during or after the conclusion of the fatigue load test.

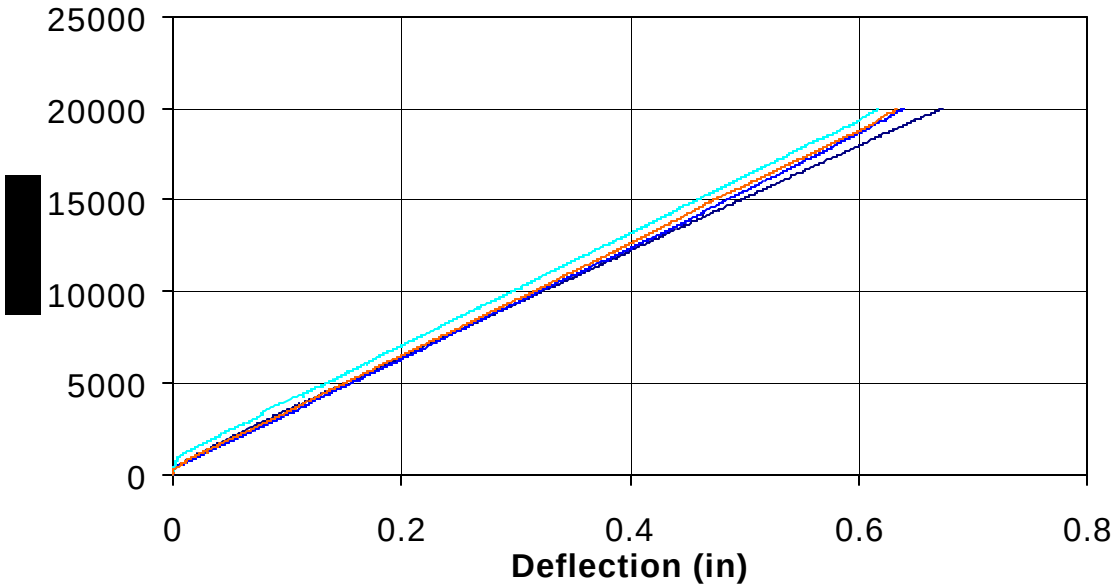

Figure 19: Load-deflection curves for progressive increments of fatigue cycles up to 2 million cycles

Note: 1 in = 25.4 mm, 1 lb = 4.45 N

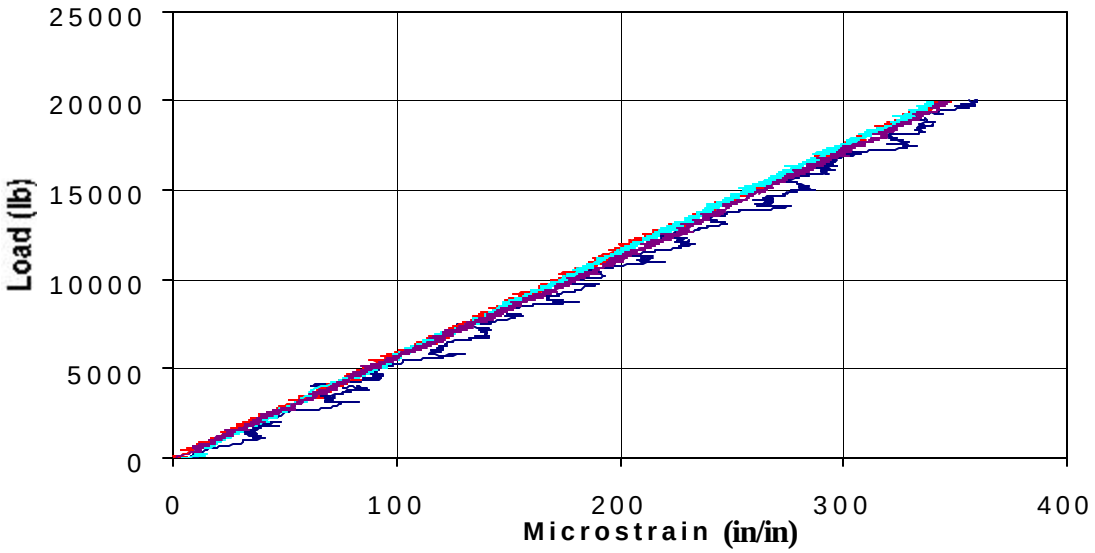

Figure 20: Load-strain curves for progressive increments of fatigue cycles up to 2 million cycles

Note: 1 in = 25.4 mm, 1 lb = 4.45 N

3.3.3 ULTIMATE LOAD TEST

The ultimate load capacity of the FRP bridge deck was performed to evaluate the overall margin of safety, the mode of failure and to provide conclusive evidence as to the strength of the bridge deck. It was tested to failure by the application of concentrated static load in cycles under four point bending configuration at the mid-span of the deck. The magnitude of the maximum load used in each successive load cycle was incremented until failure of the deck was achieved. Based on the experience of tests performed previously on a four-layered FRP tube assembly, it was expected that a few tubes of the top-most layer might pop out due to the high compressive force on them. As a precaution against any damage caused by such a type of failure, two long wooden pieces were placed on the top surface of the deck and were chained to it. The test setup has been described in detail in previous sections.

The test consisted of three loading cycles with the first two cycles resulting in some damage to the deck and failure of the sample being attained in the last cycle. The loading cycles were approximately from 0 to 88.96 kN (20,000 lb), 88.96 kN (20,000 lb) to 133.45 kN (30,000 lb) and the final cycle was from 111 kN (25,000 lb) to 155.69 kN (35,000 lb). The load versus center deflection and strain for the three cycles has been shown in Figures 21 and 22 respectively. During the fatigue test, the sample had already been tested six times under static loading up to a load of 88.96 kN (20,000 lb). So the first cycle did not result in any significant measurable, visible, or audible damage to the deck panel. The graphs clearly demonstrate that the deck had a fairly good linear elastic behavior during this cycle. It shows a consistent response on the reverse cycle with almost no loss in stiffness of the deck. The data show that the deflection of the sample at

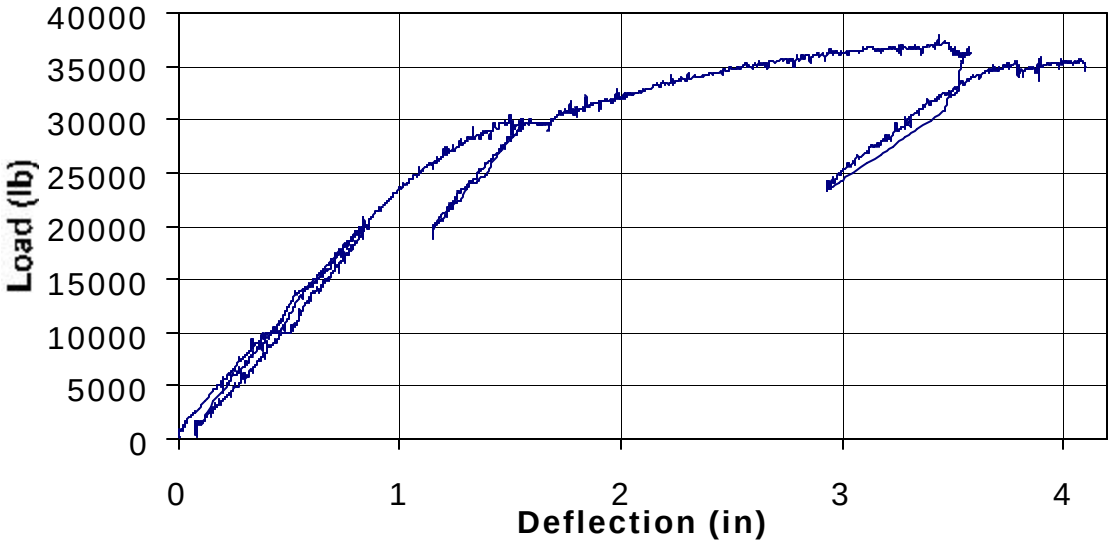

Figure 21: Load-deflection curve from ultimate load test at center

Note: 1 in = 25.4 mm, 1 lb = 4.45 N

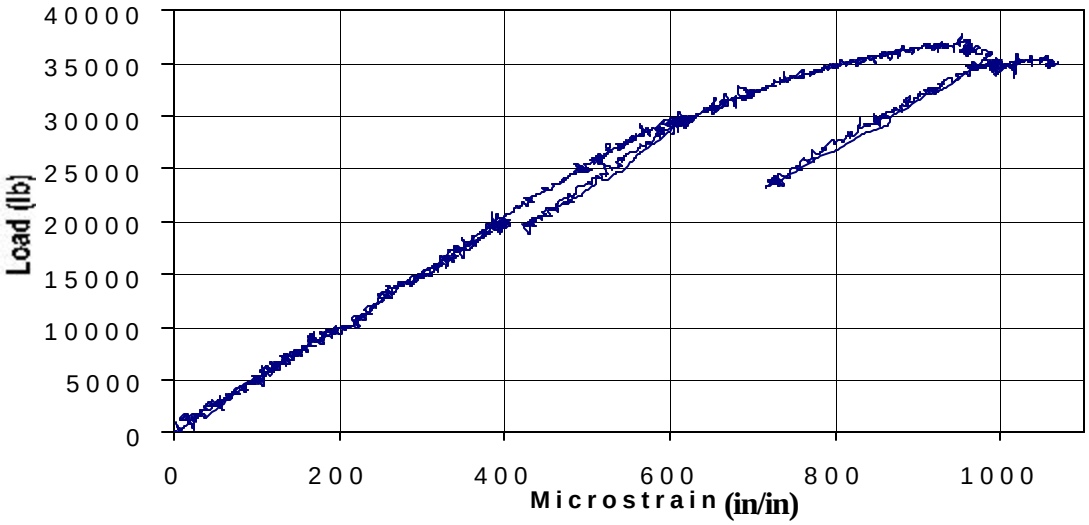

Figure 22: Load-strain curve from ultimate load test at center

Note: 1 in = 25.4 mm, 1 lb = 4.45 N

the design load of 35.5 kN (8,000 lb) was 7.9 mm (0.31 in) which was slightly more than that recorded for the design load test, but was still much below the maximum allowable deflection of 11.4 mm (0.45 in). The next two load cycles were the ones during which damage to the deck sample was observed. During the second cycle, the deflection of the test sample became prominent and could be easily perceived by visible observation. As loading was done beyond 111 kN (25,000 lb), slight twisting of tubes of the fifth layer was observed. These tubes, laid down transversely to the direction of traffic and forming a part of neck of the bridge I section, were aligned along the neutral axis of the deck structure. These tubes were acted upon by compressive loading on its top surface and by tensile loading on its bottom surface. This resulted in a twisting motion of the tubes in this layer. The shape of the tubes changed from square to a parallelogram. The tubes at the two ends of the deck sample were most affected by the twisting motion. Considerable noise was heard as the load reached around 133.45 kN (30,000 lb) and the load was promptly reduced. Upon reloading, the deck demonstrated a loss in stiffness. As the load was increased beyond 133.45 kN (30,000 lb), significant damages were observed. In the fifth layer, the tubes at the ends of the test sample showed considerable twisting. Due to this twisting motion, breaking and cracking of the fibers at the corners of the tubes was noticed. This is clearly shown in Figure 23, which is an exploded view of a few tubes in the fifth layer. The noise coming from the sample had increased considerably. It was observed that beyond the load of 169 kN (38,000 lb), the deflection was increasing without any increase in the load on the sample. The loading had severely damaged the FRP tubes in the fifth layer of the deck leading to a substantial reduction in the load carrying capacity of the whole structure. At this point the load on top of the sample was

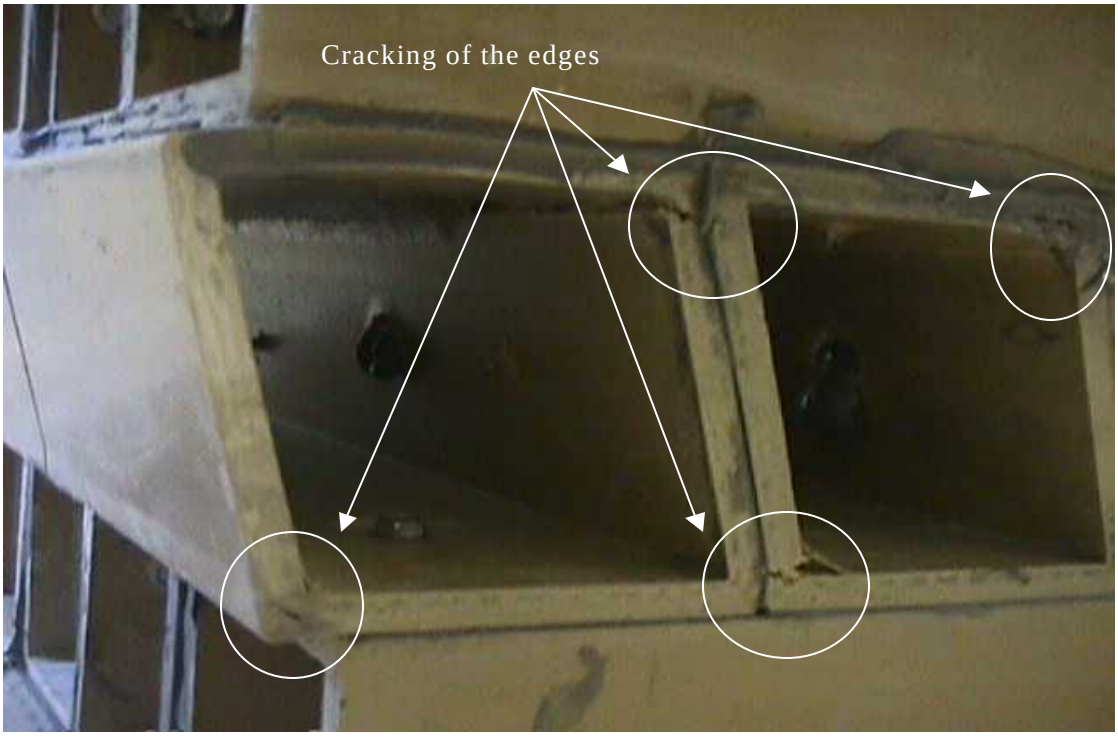

Figure 23: Exploded view of a few tubes in the fifth layer of the deck

again reduced to about 111 kN (25,000 lb). On reloading, the sample demonstrated substantial reduction in the stiffness. On reaching a load of 155.69 kN (35,000 lb) upon reloading it was noticed that the deflection and strain on the sample was increasing while the load on it remained constant. At this point it was decided that failure of the sample had been achieved and the test was stopped. On releasing the load from on top of the deck, it went back to almost its initial height. Other than the cracks and broken fibers along the corners of the tubes in the fifth layer, there was no other permanent distortion of the deck.

Unlike several other structures made out of conventional materials, the failure of the deck did not result in its total collapse and it exhibited limited but safe post-failure reserve strength. This behavior may be considered to be favorable for civil engineering designs, as the failure was not truly catastrophic. On releasing the load from on top of the deck, it went back almost to its initial height showing the flexibility or ductility of the composite material. The mode of failure observed was transverse shear failure resulting in the delaminations and cracking of fibers along the edges of the FRP pultruded tubes. It may be noted that failure was accompanied by little or no visible sign of failure of the bolts or adhesive failure between the adjacent tubes. The graphs of deflection and strain against the applied load for the failure test clearly shows the linear and non-linear behaviors of the deck at different stages of the loading. The sample demonstrated fairly good linear elastic behavior up to a load of 133.45 kN (30,000 lb). Beyond this load the deck behavior became non-linear and it started losing its stiffness. The largest overall longitudinal strain recorded during this test was 1071 microstrain, located at the center of bottom surface of the deck. Figure 24 shows the plot of the longitudinal strain recorded

on the tubes of the second layer, directly under the loading patch. The tubes in this layer were under compression with the maximum of –736 microstrain. The extensive area under the load-deflection curve in Figure 21 indicates that the FRP deck has excellent energy absorption capability.

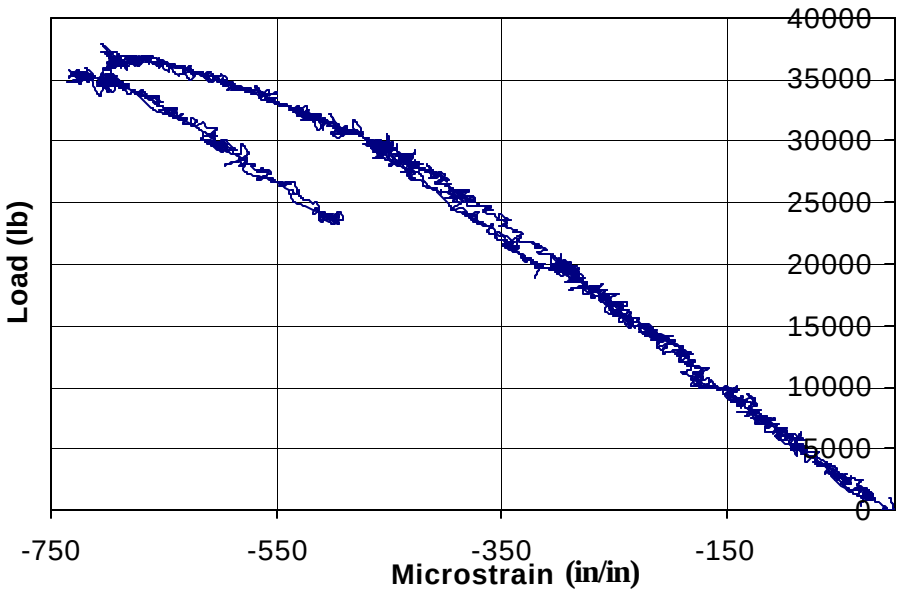

Figure 24: Plot of longitudinal strain recorded on the tubes of second layer directly below the loading patch

Note: 1 in = 25.4 mm, 1 lb = 4.45 N

3.4 EVALUATION OF DECK PERFORMANCE

The results of the three different tests performed on the prototype deck sample were used to determine characteristics of the full-size bridge deck. The test sample failed at about 155.69 kN (35,000 lb), which is of the order of four times the design wheel load for a quarter portion of the deck. This indicates extremely good performance of the deck as far as strength is concerned. The mid-span deflections of the deck sample at the design wheel load were 6.6 mm (0.26 in) and 7.9 mm (0.31 in) for the static test before fatigue loading and the post-fatigue ultimate load test respectively. These mid-span deflections of the deck sample were well within the 11.4 mm (0.45 in) range, which is the maximum deflection based on length/800 design criteria specified by AASHTO guidelines. From observations made during the test and on analyzing the failure mode, it can be concluded that the load carrying capacity of the deck can be increased by preventing the twisting of tubes in the fifth layer from the top of the deck. The performance of the test sample with regards to AASHTO strength and deflection requirements was much better then anticipated. Taking the test results into consideration, it was decided to remove the topmost layer of GFRP tubes from the full-size bridge deck, leading to reduction in the material, thickness, weight, and cost of the deck while still meeting the AASHTO requirements.

3.5 BRIDGE INSTALLATION

The bridge was installed at UMR campus on July 29, 2000 (See Figure 25 and Figure 26). The bridge is equipped with integral fiber optic sensors and the response of the bridge will be remotely monitored.

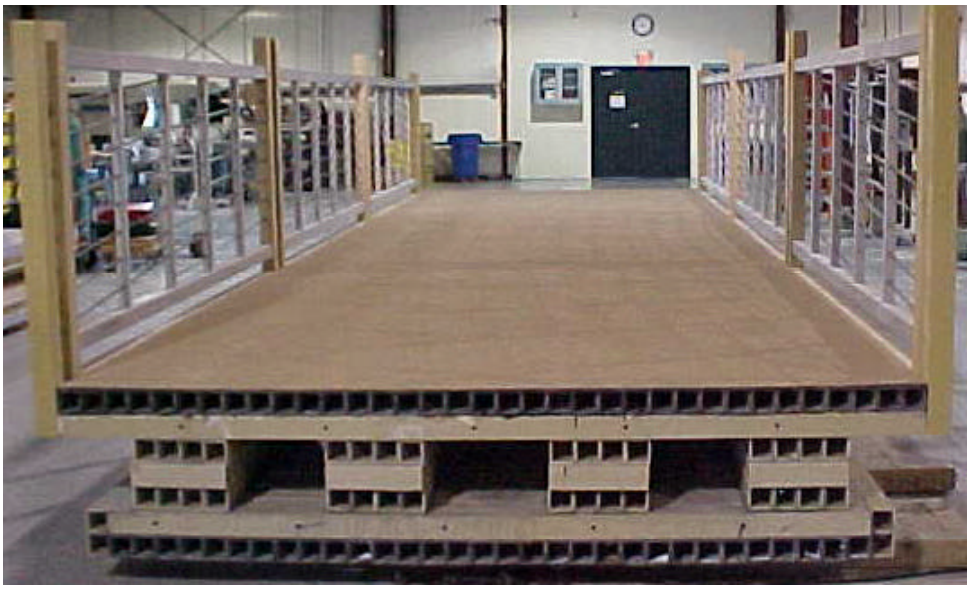

Figure 25: Assembled composite bridge

Figure 26: Installation of bridge deck

4. CONCLUSIONS

Testing of the prototype quarter portion of the bridge deck indicates that the design of bridge deck using readily available, off-the-shelf pultruded glass and carbon FRP tubes can meet the necessary strength and deflection design criteria as defined in the AASHTO specifications.

The deflection and strain histories show linear elastic bending and shear behavior with a slightly non-linear envelope close to the failure load. The deflections and strains are very symmetric up to the point of failure. The net central deflection ranged within the allowable limits of length/800.

The fatigue test served as simple baseline indicator of the long-term durability of the composite deck. The sample showed almost no reduction in stiffness or strength after 2 million cycles of fatigue loading in excess of the design wheel load.

The failure load of 133.45 kN (30,000 lb) was almost four times the design wheel load of 35.5 kN (8,000 lb) for the quarter section of the bridge deck. The failure was caused due to the twisting of tubes in the fifth layer from top of the deck while at the same time almost no other form of distortion or failure was observed in any other layer of tubes. Damage accumulated gradually at higher load levels, which is reflected in the deflection and strain histories. Ultimate failure was non-catastrophic which is advantageous from a civil engineering point of view.

The testing of quarter portion of the bridge deck in the laboratory provided valuable information to resolve certain manufacturing and design issues such as bonding between the tubes and number of layers of tubes to be used. Furthermore, the data

measured during the testing provided baseline information by which to judge the bridge design and to compare later test data from the actual installed full-size bridge deck.

Based on results of the present research and of extensive laboratory tests on FRP tubes and their assemblies, all-composite bridge decks made of pultruded glass and carbon tubes are judged to be a suitable replacement for short span bridges made of conventional materials. Although this is not the most efficient design for an all-composite bridge deck, it does represent a unique opportunity to implement composites in a vehicular bridge.

5. RECOMMENDATIONS

A number of issues still need to be investigated for optimizing the present bridge design. The following are the recommendations based on the investigations conducted within the scope of this project:

- The reason for failure of the test sample was due to the twisting of tubes in the fifth layer of the deck sample. This twisting motion caused the tubes to lose their shape and also lead to cracking of the fibers along the edges of the tubes. To prevent this twisting motion and hence the cracking, pultruded tubes with improved transverse properties are required.
- The ultimate load capacity of the deck can be increased by replacing the fifth layer of GFRP tubes, laid down transversely to the direction of the traffic, with GFRP tubes running lengthwise along the deck. This will result in providing more strength and stiffness to the deck as the longitudinal tubes in the fifth layer will then be one of the main load bearing members.
- In order for the all-FRP bridge deck to behave monolithically, adequate bonding between the FRP tubes is necessary. To ensure this, further investigation into the long term performance is required with regard to the adhesive used for bonding the tubes.
- Durability results and sensor data from tests with live loads should be used to provide information required for determining the cost-effective measures to be used in life-cycle planning, determining a maintenance strategy, and establishing guidelines for composite bridges for use in the transportation infrastructure.

6. REFERENCES

Agarwal, B. D. and Broutman, L. J. (1990), "Analysis and Performance of Fiber Composites", John Wiley & Sons, Inc.

American Association of State Highway and Transportation Officials. (1996). "Standard Specifications for Highway Bridges", AASHTO, Washington D.C., Sixteenth Edition.

Ballinger, C. A. (1990). "Structural FRP composites-Civil Engineering's Material of the Future?", Civil Engineering, ASCE, 60(7), pp. 63-65.

Bank, L. C., (1989). "Properties of Pultruded Fiber Reinforced Plastic Structural Members", Transportation Research Record 1223, Transportation Research Board, Washington D.C., pp. 117-124.

Barbero, E. J., Fu, S. H. and Raftoyiannis, I. (1991). "Ultimate Bending Strength of Composite Beams", Journal of Materials in Civil Engineering, Vol. 3, No. 4, November, pp. 292-306.

Chajes, M., Gillespie, J., Mertz, D., Shenton, H. (1998). "Advanced Composite Bridges in Delaware", Proceedings of Second International Conference on Composites in Infrastructure, Tuscon, Arizona, Vol. 1, January 5-7, pp. 645-650.

Davalos, J. F., and Qiao, P. (1997). "Analytical and Experimental Study of Lateral and Distortional Buckling of FRP Wide-Flange Beams", Journal of Composites for Construction, Vol. 1, No. 4, pp. 150-159.

Fisher, S., Roman, I., Harel, H., Marom, G., and Wagner, H. D. (1981). "Simultaneous Determination of Shear and Young's Moduli in Composites", Journal of Testing and Evaluation, Vol. 9, No. 5, September, pp. 303-307.

Foster, D. C., Goble, G. C., Schulz, J. L., Commander, B. C., and Thomson, D. L. (1998). "Structural Testing of a Composite Material Highway Bridge", Proceedings of International Composites Expo, Session 4-C, pp. 1-9.

Fu, S. H., Spyrakos, C., Prucz, J., and Barbero, E. J. (1990). "Structural Performance of Plastic I-Beams", Proceedings of Eighth Annual Structures Congress, ASCE, pp. 507-508

Head, P. R. (1992). "Design Methods and Bridge Forms for the Cost Effective use of Advanced Composites in Bridges", Proceedings of 1st International Conference of Advanced Composite Materials in Bridges and Structures, Sherbrooke, Quebec, Canada, pp. 15-30.

Liskey, K. (1991). "Structural Applications of Pultruded Composite Products", Proceedings of Specialty Conference on Advanced Composite Materials in Civil Engineering Structures, Las Vegas, NV, January 31 & February 1, ASCE, New York, N.Y., pp. 182-193.

Lopez-Anido, R., Gangarao, H. V. S., Pauer, R. J., and Vedam, V. R. (1998a). "Evaluation of Polymer Concrete Overlay for FRP Composite Bridge Deck", Proceedings of International Composites Expo, Session 13-F, pp. 1-6.

Lopez-Anido, R., Howdyshell, P. A., Stephenson, L. D., and Gangarao, H. V. S. (1998b). "Fatigue and Failure Evaluation of Modular FRP Composite Bridge Deck." Proceedings of International Composites Expo, Session 4-B, pp. 1-6.

Nagraj, V. and Ganga, Rao, H. V. S. (1993). " Characterization of GFRP Pultruded Box Beams Under Static and Fatigue Loads", SAMPE Quarterly (Journal of Advanced Materials), Vol. 24, No. 4, pp. 3-9.

Nagraj, V., and Ganga, Rao, H. V. S. (1997). "Static Behavior of Pultruded GFRP Beams", Journal of Composites for Construction, Vol. 1, No. 3, August, pp. 120-129.

Plunkett, J.D. (1997). "Fiber-Reinforced Polymer Honeycomb Short Span Bridge for Rapid Installation", IDEA Project Final Report, Contract NCHRP-96-ID030, Transportation Research Board, National Research Council.

Richards, D., Dumlao, C., Henderson, M., and Foster, D. C. (1998). "Methods of Installation and the Structural Analysis of Two Short Span Composite Highway Bridges", Proceedings of International Composites Expo, Session 4-E, pp. 1-6.

Seible, F. (1998). "US Perspective of Advanced Composites Bridge Technology in Europe and Japan", Proceedings of Second International Conference on Composites in Infrastructure, Vol. 2, January 5-7, pp. 605-636.

Sotiropoulos, S. N., Gangarao, H. V. S., and Allison, R. W. (1994). "Structural Efficiency of Pultruded FRP Bolted and Adhesive Connections", Proceedings of 49th Annual Conference, Composite Institute, The Society of Plastics Industry Inc., Cincinnati, Ohio, SPI/Composite Institute, New York, N.Y.

Zureick, A. H., Shih, B., and Munley, E. (1995). "Fiber-Reinforced Polymeric Bridge Decks", Structural Engineering Review, Vol. 7, No. 3, pp. 257-266.